Volume 3 Issue 2

# MERSIN PHOTOGRAMMETRY JOURNAL

**The MERSİN PHOTOGRAMMETRY JOURNAL (MEPHOJ)**

THE MERSİN PHOTOGRAMMETRY JOURNAL (MEPHOJ) publishes original and innovative contributions in photogrammetric applications ranging from the integration of instruments, methodologies, and technologies and their respective uses in the environmental sciences, engineering, and other natural sciences. Mersin Photogrammerty Journal is a branch of science that widely applied in many scientific disciplines. MEPHOJ aims to cover the entirety of Photogrammetry and Photogrammetric aplications about Geosciences, including their application domains. MEPHOJ strives to encourage scientists to publish experimental, theoretical, and computational results as detailed as possible so that results can be easily reproduced.

MEPHOJ is a double peer-reviewed (blind) OPEN ACCESS JOURNAL that publishes professional level research articles and subject reviews exclusively in English. It allows authors to submit articles online and track his or her progress via its web interface. All manuscripts will undergo a refereeing process; acceptance for publication is based on at least two positive reviews. The journal publishes research and review papers, professional communication, and technical notes. MEPHOJ does not charge for any article submissions or for processing.

CORRESPONDENCE ADDRESS
Journal Contact: myakar@mersin.edu.tr

# CONTENTS

*Volume 3 - Issue 2*

## RESEARCH ARTICLES

**Mersin Photogrammetry Journal**

https://dergipark.org.tr/en/pub/mephoj

**e-ISSN 2687-654X**

# 3D model of Üçayak Ruins obtained from point clouds

**Aydın Alptekin*[1], Murat Yakar[2]**

[1]Mersin University, Engineering Faculty, Geological Engineering Department, Mersin, Turkey
[2]Mersin University, Engineering Faculty, Geomatics Engineering Department, Mersin, Turkey

**Keywords**
Cultural heritage
UAV
3D Model
Photogrammetry
Circular mission plan

**ABSTRACT**

Historical artifacts are in danger all over the world as they are being damaged continuously. In order to transfer them to future generations and restore them, we need to create digital products of them. The developments in remote sensing allow us to model objects in computer environment. In this study, a cultural heritage located in Mersin was modelled in 3D using an unmanned aerial vehicle (UAV). Circular mission plan in the mobile phone application was preferred. Overlapping pictures were aligned. Digital surface model, orthophoto and 3D model of Ucayak Ruins have been created. Aerial photogrammetry allows us to create digital products in a short time. The obtained model will be used in tourism advertisements.

## 1. Introduction

Turkey has hosted many civilizations throughout history. Turkey has been preferred for settlement because it is surrounded by the sea on three sides, is located on migration routes and has fertile agricultural lands. Assyrians, Byzantine, Seljuk and Ottoman Empires have lived in this territory. These civilizations have left us cultural legacies. As a result, Turkey has a deep history of geoarchaeological sites.

Mersin City, located in the southern parts of Turkey, has a great potential for archeological studies (Alptekin and Yakar 2021). There are many archaeological study areas such as Kızkalesi, Olba Ancient City, Anemurium, Heaven Hell Potholes and Uzuncaburç. They are being negatively affected from natural and anthropogenic effects.

Geopark turizm has been gaining importance since last decade. Geoparks occur with the process of million years. Mut Miocene Basin is one of the candidates Geopark sites in Turkey. Moreover, it has canyon, valley, and waterfall in it. Geoparks are open air laboratories to describe geological events.

Agriculture and tourism are the main incomes of Mersin. Geo-tourism is important for rural development of Turkey (Kocalar, 2020; Varol et al. 2021). However, Mersin is experiencing a lack of publicity.

Historical artifacts are important sources that enable us to reach the life information of the past (Yakar et al. 2005; Yakar et al. 2010). However, they are being damaged due to the unconscious behaviors of people, treasure hunters, natural disasters and climate changes (Ulvi and Yakar, 2010). We need to document our cultural heritage in the computer environment, in order to pass it on to future generations, use it in tourism and restore it in the future (Yakar et al. 2016).

Terrestrial laser scanner (TLS) and unmanned aerial vehicle (UAV) have been used to model the archeological sites in 3D since last decade. Alptekin et al. 2019 have used TLS to model the mausoleum in Kanlıdivane.

In this study, Üçayaklı ruins located in Erdemli province of Mersin city was modeled using a UAV. Üçayaklı ruins, also called villa rustika, was the residence of the great landowners during the Roman and Byzantine periods. The walls of the building, which has been well preserved until today, are intact. However, the ceiling and floor, which was made of wooden, were demolished (Çalışkan et al.2009). The

* **Corresponding Author**

*(aydinalptekin@mersin.edu.tr) ORCID ID 0000-0002-5605- 0758
(myakar@mersin.edu.tr) ORCID ID 0000 – 0002 – 2664 – 6251

**Cite this article**

Alptekin A & Yakar M (2021). 3D model of Üçayak Ruins obtained from point clouds. Mersin Photogrammetry Journal, 3(2), 37-40

**Research Article / DOI: 10.53093/mephoj.939079**

**Received: 18/05/2021; Accepted: 23/09/2021**

second floor has large windows and consoles that prove the presence of a balcony, while the first floor has small windows (Fig.1).

**Figure 1.** Ucayak ruins

## 2. Study area

Mersin is located between Mediterrenean Sea and Taurus Mountains. The study area is located in Erdemli Disrict, Mersin Province (Figure 2). Ucayak Ruins is between Küstülü and Hüsametli villages. Total distance to Mersin city center is 65 km.

**Figure 2.** Location map

## 3. Methods

UAV has been frequently used in engineering projects since last decade. UAV has been used in agriculture (Bendig et al. 2014; Şenol et al. 2021), culture heritage modelling (Şasi and Yakar, 2018; Ulvi et al. 2019; Sarı et al. 2020), mapping landslide area (Al-Rawabdeh et al. 2017; road extraction (Yiğit and Uysal, 2021), shoreline change detection (Unel et al. 2019), pond volume measurement (Alptekin and Yakar 2020).

Obtaining accurate and complete data will increase the accuracy of the documentation work (Hamal et al. 2020). Visual and scientific applications of 3D modelling have a great role in documentation of cultural heritage (Yılmaz et al. 2008). Terrestrial photogrammetry is not able to take pictures from the roof of the structure. Aerial photogrammetry will solve this problem. Therefore, aerial photogrammetry will be selected in building modelling projects.

There are many softwares such as Agisoft, ContextCapture and Photomodeller that can model the object in 3D. Kabadayı et al. 2020 have discussed the advantages and disadvantages of these softwares.

In this study, Anafi Parrot (Figure 3) has been used to take pictures of cultural heritage. Technical properties of Anafi Parrot is given in Table 1.

**Figure 3.** Anafi Parrot

**Table 1.** Technical properties of Anafi Parrot

| Property | Value |
|---|---|
| Drone weight | 320 g |
| Controller weight | 386 g |
| Battery weight | 126 g |
| Max. flight time | 25 min |
| Max. horizontal speed | 15.2 m/s |
| Max. vertical speed | 4 m/s |
| Max. wind resistance | 13.9 m/s |
| Max. transmission range | 4000 m |
| Max. altitude | 150 m |
| Operating temperature range | -10 C° to 40 C° |
| Camera | 21 MP |
| Resolution | 4608x3456 |
| Focal length | 4 mm |
| Pixel size | 1.34 x 1.34 µm |

Pix4Dcapture, a cell phone application, has been used to prepare circular mission flight plan. The flight height was 30m and GSD was 3.87 cm/pixel. Circular mission plan is used to take pictures of an object with 3D. In this study, 107 overlapping pictures were taken (Figure 4). The pictures were processed in Agisoft Metashape software 1.5.0. The steps is shown in Fig. 5.

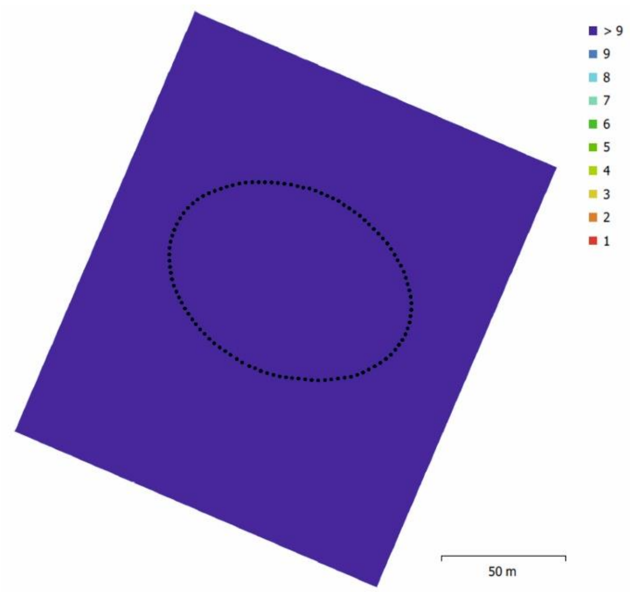


**Figure 4.** Camera locations

Add Photos
Convert coordinates of photos
Align Photos
Build mesh
Add ground control points
Input marker coordinates
Optimize camera
Build dense cloud
Build mesh
Build texture
Generate orthophoto
Generate DSM

**Figure 5.** Process steps

To georeference the study area, four ground control points were used. Coordinates were taken by using a GPS with one epoch. Error amounts are given in Table 2.

**Table 2.** Error amounts of ground control points

| Direction | Error amount (mm) |
|---|---|
| X error | 6.19458 |
| Y error | 3.87626 |
| Z error | 4.81898 |
| XY error | 7.30741 |
| Total | 8.75333 |

## 4. Results

In this study, 3D model was created with medium quality (Fig 6). High quality model needs high standards of computer. Moreover, pictures taken from close-range will increase the resolution of the model.

DSM (Fig. 7) and orthophoto (Fig. 8) of the study area were created. The elevation of the study area is between 906 and 928 meters. Orthophoto has too many white holes because of circular mission flight plan.

**Figure 6.** 3D Model

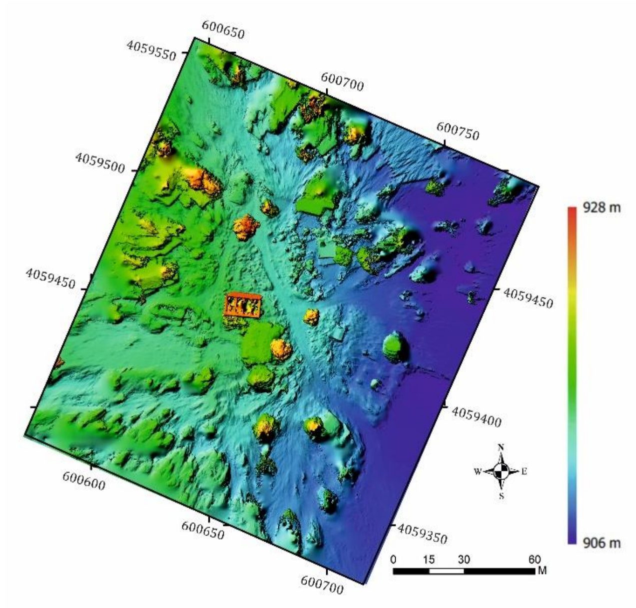


**Figure 7.** DSM

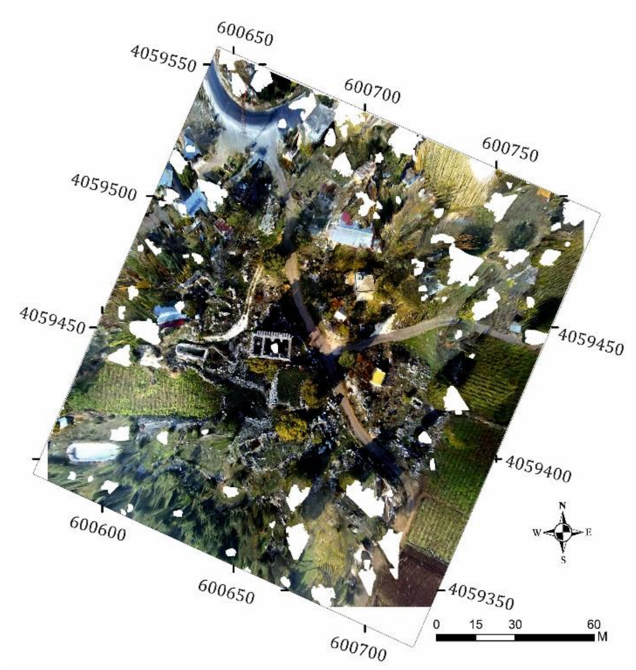


**Figure 8.** Orthophoto

## 5. Discussion

It is very important to transfer historical artifacts bearing the signatures of world history to future generations (Yakar et al. 2015). Along with the developing technology, the classical method of documentation has now been replaced by modern documentation techniques, which has led to the rapid advancement of contemporary documentation techniques (Korumaz et al. 2011).

In today, modelling of a cultural heritage is being performed with using a UAV. The pictures will be taken manually with a UAV. Overlapping pictures will be aligned with the help of tie points. The quality of the model will be increased when high quality aligned mode is selected.

Circular mission plan is an alternative to manually taken pictures. It will be used easily in Pix4Dcapture mobile application.

## 6. Conclusion

Historical artifacts are in danger all over the world. Turkey has an ancient history. Too many civilizations have lived and left us precious cultural heritages. Documenting historical artifacts is vital to transfer cultural heritage to future generations. Modern technology allows us to create 3D model of the object with high accuracy in a short time. In this study, the model of Ucayak Ruins has been created in 3D. This model will be used in tourism advertisements.

**Author contributions**

**Aydın Alptekin:** Literature review, Field study, Modelling, Writing; **Murat Yakar:** Editing

**Conflicts of interest**

The authors declare no conflicts of interest.

**References**


Alptekin A & Yakar M (2020). Determination of pond volume with using an unmanned aerial vehicle. *Mersin Photogrammetry Journal*, *2*(2), 59-63.

Alptekin A & Yakar M (2021). İçel İli jeolojisine ve jeolojik sorunlarına genel bir bakış. *İçel Dergisi*, *1*(1), 27-30.

Alptekin A, Çelik M Ö & Yakar M (2019). Anıtmezarın yersel lazer tarayıcı kullanarak 3B modellenmesi. *Türkiye Lidar Dergisi*, *1*(1), 1-4.

Al-Rawabdeh A, Moussa A, Foroutan M, El-Sheimy N & Habib A (2017). Time series UAV image-based point clouds for landslide progression evaluation applications. *Sensors*, *17*(10), 2378.

Bendig J, Bolten A, Bennertz S, Broscheit J, Eichfuss S & Bareth G (2014). Estimating biomass of barley using crop surface models (CSMs) derived from UAV-based RGB imaging. *Remote sensing*, *6*(11), 10395-10412.

Çalışkan M, Aydın A, Aydınoğlu Ü & Kerem F (2009). *Mersin: ören yerleri, kaleleri, müzeleri*. İl Özel İdaresi.

Hamal S N G, Sarı B & Ulvi A (2020). Using of Hybrid Data Acquisition Techniques for Cultural Heritage a Case Study of Pompeiopolis. *Türkiye İnsansız Hava Araçları Dergisi*, *2*(2), 55-60.

Kabadayı A, Yunus K & Yiğit A Y (2020). Comparison of documentation cultural artifacts using the 3D model in different software. *Mersin Photogrammetry Journal*, *2*(2), 51-58.

Kocalar A C (2020). LATMOS GEOPARK (BEŞPARMAK MOUNTAINS) WITH HERAKLEIALATMOS ANTIQUE HARBOUR CITY AND BAFA LAKE NATURAL PARK IN TURKEY. *Turkish Journal of Engineering*, *4*(4), 176-182.

Korumaz A G, Dülgerler O N & Yakar M (2011). KÜLTÜREL MİRASIN BELGELENMESİNDE DİJİTAL YAKLAŞIMLAR. *Selçuk Üniversitesi Mühendislik, Bilim ve Teknoloji Dergisi*, *26*(3), 67-83.

Sarı B, Hamal S N G & Ulvi A (2020). Documentation of complex structure using Unmanned Aerial Vehicle (UAV) photogrammetry method and Terrestrial Laser Scanner (TLS). Türkiye Lidar Dergisi, 2(2), 48- 54

Şasi A & Yakar M (2018). Photogrammetric modelling of hasbey dar'ülhuffaz (masjid) using an unmanned aerial vehicle. *International Journal of Engineering and Geosciences*, *3*(1), 6-11.

Şenol H İ, Yiğit A Y, Kaya Y & Ulvi A (2021). İHA ve yersel fotogrametrik veri füzyonu ile kültürel mirasın 3 boyutlu (3B) modelleme uygulaması: Kanlıdivane Örneği. Türkiye Fotogrametri Dergisi, 3(1), 29-36.

Ulvi A & Yakar M (2010). An experimental study on preparing photogrammetric rolove plans of antique theatres. *International Journal of the Physical Sciences*, *5*(7), 1086-1092.

Ulvi A, Yakar M, Yiğit A & Kaya Y (2019). The Use of Photogrammetric Techniques in Documenting Cultural Heritage: The Example of Aksaray Selime Sultan Tomb. *Universal Journal Of Engineering Science*, *7*(3), 64-73.

Ünel F B, Kuşak L, Çelik M Ö, Alptekin A & Yakar M (2020). Kıyı Çizgisinin Belirlenerek Mülkiyet Durumunun İncelenmesi. *Türkiye Arazi Yönetimi Dergisi*, *2*(1), 33-40.

Varol F, Yiğit A Y & Ulvi A (2021). Kültürel Mirasın Dijital Ortamda 3 Boyutlu Arşivlenmesi: Maghoki-Attar Camii Sanal Model Örneği. Turizm Akademik Dergisi, 8 (1), 181-191.

Yakar M, Kabadayı A, Yiğit A Y, Çıkıkcı K, Kaya Y & Catin, S. S. (2016). Emir Saltuk Kümbeti Fotogrametrik Rölöve Çalişmasi ve 3Boyutlu Modellenmesi. *Geomatik*, *1*(1), 14-18.

Yakar M, Orhan O, Ulvi A, Yiğit A Y & Yüzer M M (2015). Sahip Ata Külliyesi Rölöve Örneği. *TMMOB Harita ve Kadastro Mühendisleri Odası*, *10*.

Yakar M, Yıldız F & Yılmaz H M (2005). Tarihi ve Kültürel Miraslarin Belgelenmesinde Jeodezi Fotogrametri Mühendislerinin Rolü. TMMOB Harita ve Kadastro Mühendisleri Odası, 10.

Yakar M, Yılmaz H M & Mutluoğlu Ö (2010). Comparative evaluation of excavation volume by TLS and total topographic station based methods. Lasers in Eng,19, 331-345.

Yiğit A Y & Uysal M (2021). Yüksek Çözünürlüklü İnsansız Hava Aracı (İHA) Görüntülerinden Karayolların Tespiti. Bitlis Eren Üniversitesi Fen Bilimleri Dergisi, 10 (3), 1040-1054. DOI: 10.17798/bitlisfen.900817

Yilmaz H M, Yakar M & Yildiz F (2008). Digital photogrammetry in obtaining of 3D model data of irregular small objects. *The International Archives of the Photogrammetry, Remote Sensing and Spatial Information Sciences*, *37*, 125-130.

*Mersin Photogrammetry Journal – 2021; 3(2); 41-47*

**Mersin Photogrammetry Journal**

https://dergipark.org.tr/en/pub/mephoj

**e-ISSN 2687-654X**

# The impacts of vegetation indices from UAV-based RGB imagery on land cover classification using ensemble learning

**Muhammed Yusuf Öztürk** [*1], **İsmail Çölkesen** [1]

[1] *Gebze Technical University, Engineering Faculty, Department of Geomatics Engineering, Kocaeli, Turkey*

**Keywords**
Ensemble learning
UAV
LULC
LightGBM
XGBoost

**ABSTRACT**

The production of land use and land cover (LULC) maps using UAV images obtained by RGB cameras offering very high spatial resolution has recently increased. Vegetation indices (VIs) have been widely used as an important ancillary data to increase the limited spectral information of the UAV image in pixel-based classification. The main goal of this study is to analyze the effect of frequently used RGB-based VIs including green leaf index (GLI), red-green-blue vegetation index (RGBVI) and triangular greenness index (TGI) on the classification of UAV images. For this purpose, five different dataset combinations comprising of RGB bands and VIs were formed. In order to evaluate their effects on thematic map accuracy, four ensemble learning methods, namely RF, XGBoost, LightGBM and CatBoost were utilized in classification process. Classification results showed that the use of RGB UAV image with VIs increased the overall accuracy (OA) values in all cases. On the other hand, the highest OA values were calculated with the use of Dataset-5 (i.e. RGB bands and all VIs considered). Additionally, the classification result of Dataset-4 (i.e. RGB bands and TGI) showed superior performance compared to Dataset-2 (i.e. RGB bands and GLI) and Dataset-3 (i.e. RGB bands and RGBVI). All in all, the TGI was found to be useful for improving classification accuracy of UAV image having limited spectral information compared to GLI and RGBVI. The improvement in overall accuracy reached to 2% with the use of RGB bands and TGI index. Furthermore, within the ensemble algorithms, CatBoost produced the highest overall accuracy (92.24%) with the dataset consist of RBG bands and all VIs considered.

## 1. Introduction

Gathering accurate and reliable land use and land cover (LULC) information about the Earth's surface is a prerequisite for the success of a wide range of applications carried out at local, regional and global scales (Colkesen and Ertekin, 2020). Recent developments in the field of unmanned aerial vehicle (UAV) technologies and imaging sensor systems have led to a renewed interest in extracting required information about surface objects from high spatial resolution UAV images (Yao and Qin, 2019).

Supervised pixel-based image classification that one of the popular classification techniques to produce LULC maps in the literature (Huth et al., 2012; Tehrany et al., 2014; Goldblatt et al., 2018). Pixel-based image classification is generally based on the assignment of the image pixels into pre-defined LULC classes using their digital numbers. The RGB-UAV-based platform is an alternative and low-cost aerial platform technology ensuring the capturing surface images at very high spatial and temporal resolutions. Although the RGB cameras are able to provide high spatial information about the surface, their spectral resolutions are limited for distinguishing spectrally similar pixels (Jang et al., 2020). In order to overcome this limitation, the ancillary data such as vegetation indices, texture features and principal components have been widely used in image classification process. Combinations of various vegetation indices (VIs) and RGB bands have been frequently used in the literature to improve the classification performance of RGB-UAV images (Sumesh et al., 2021). Many vegetation indices based on different sensor specifications have been developed since the launch of the first remote sensing satellite, Landsat. They are widely used for quantitative and qualitative evaluations of vegetation information (Xue and Su, 2017).

* **Corresponding Author**

*(m.ozturk2020@gtu.edu.tr) ORCID ID 0000 – 0001 – 6459 – 9356
(icolkesen@gtu.edu.tr) ORCID ID 0000 – 0001 – 9670 – 3023

**Research Article / DOI: 10.53093/mephoj.943347**

**Cite this article**

Öztürk M Y & Çölkesen İ (2021). The impacts of vegetation indices from UAV-based RGB imagery on land cover classification using ensemble learning. Mersin Photogrammetry Journal, 3(2), 41-47

**Received: 26/05/2021; Accepted: 28/08/2021**

Choosing the most appropriate classification algorithm for classifying UAV images having limited spectral information is also one of the important factors effecting the thematic map accuracy. In recent years, there has been great interest in classifying digital images using ensemble learning methods in the literature due to their robust, effective and fast performance (Zhiwei et al., 2016). The main idea behind the ensemble learning is to combine predictions of multiple learners (e.g. decision trees) to final decision on a given unknown sample (Tonbul et al., 2020). Previous studies confirmed that decision tree based ensemble learning algorithms such as bagging, boosting, RF, XGBoost, LightGBM and CatBoost perform better than utilize of single decision tree classifier (Sagi and Rokach, 2018; Shi et al., 2021).

The main purpose of this study is to analyse the effect of the use of RGB based vegetation indices on the LULC classification accuracy. For this purpose, three widely preferred vegetation indices, namely green leaf index (GLI), red-green-blue vegetation index (RGBVI) and triangular greenness index (TGI) were formed as ancillary dataset. RF, XGBoost, LightGBM and CatBoost ensemble learning algorithms were utilized to perform classification process. Classification results were evaluated using overall accuracy (OA), Kappa coefficient and F-score measures.

## 2. Study area and dataset

The study area covers the north-eastern part of Gebze Technical University located in Gebze district of Kocaeli province. As shown in Figure 1, within the boundaries of the study area, faculty buildings, other man-made structures, green vegetation and bare soil areas exist. Study area consists of six main LULC classes: concrete including gray stone floor, road, gray and white roofs, forest class including deciduous trees, coniferous trees and grass, parkour including bicycle road, basketball and tennis court, shadow, soil and tile roof.

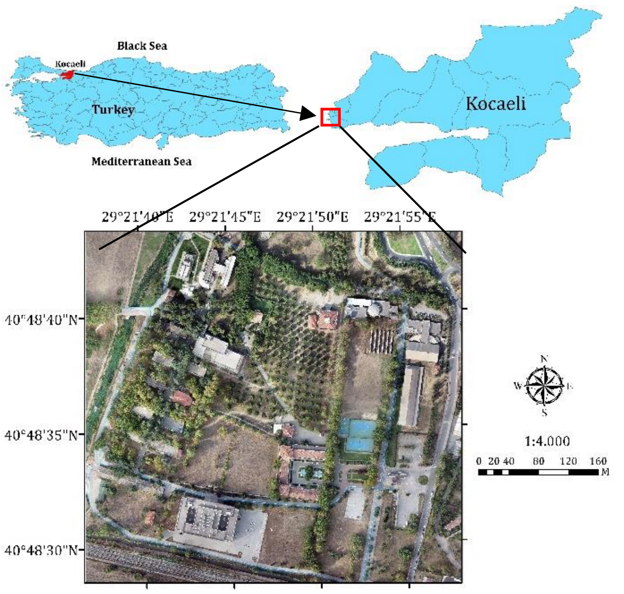


**Figure 1.** Study area

In this study, UAV-based high-resolution remote images were acquired on 24 September 2020 by Phantom IV Pro V2.0 drone equipped with a 20 MP RGB camera (Table 1). "Pix4Dmapper" application was preferred for flight planning. The images collected from 80 m flight altitude with 80% forward overlap and %70 side overlap, resulting in ground sampling distance 2.3 cm. Agisoft PhotoScan software was used to process the obtained images and as a result, an 8-bit ortho-mosaic with a spatial resolution of 5 cm was produced.

**Table 1.** Specifications of Phantom IV Pro V2.0

| Technical Specifications | Value |
|---|---|
| Sensor | 1 inch 20MP |
| Weight | 1375 gr |
| Max Flight Time | 30 min |
| Max Speed | 45 mph (72 km/h) |
| Max Ascent Speed | 6 m/s |
| Max Descent Speed | 4 m/s |
| GNSS Module | GPS/GLONASS |
| Hover Accuracy Range | Vertical: ±0.1 m<br>Horizontal: ±0.3 m |

## 3. Methodology

In this study, the effect of the use of RGB based GLI, RGBVI and TGI vegetation indices on the accuracy of thematic maps produced from UAV image were analyzed. For this purpose, training and validation pixels for each LULC classes were determined on UAV images. Four robust ensemble learning algorithms, namely, RF, XGBoost, LightGBM and CatBoost, were utilized to construct classification model using training samples. Then, the datasets consisting of the combinations of UAV images and vegetation indices were classified with the constructed classification models and thematic maps were produced. In order to conduct the accuracy assessment, OA, kappa coefficient and F-scores were utilized, and derived results analyzed.

### 3.1. Vegetation indices (VIs)

VIs are obtained from the mathematical equations applied to two or more spectral bands to emphasize the vegetation characteristics. Various VIs based on RGB bands have been developed. In this study, GLI, RGBVI and TGI indices, frequently used in various studies in the literature, were evaluated.

GLI was developed by the Louhaichi et al. (2001) for determination of wheat planted areas using 8-bit RGB camera. GLI values take values between -1 and +1. Negative values correspond to soil and lifeless features, whereas positive values correspond to green vegetation.

$$GLI = \frac{2 \times Green - Red - Blue}{2 \times Green + Red + Blue} \quad (1)$$

RGBVI was developed for biomass estimation by Bendig et al. (2015). It can be described as the normalized difference of the squared green spectral band and the product of blue×red bands.

$$RGBVI = \frac{Green^2 - Blue \times Red}{Green^2 + Blue \times Red} \quad (2)$$

TGI, based on red, green and blue spectral bands, is sensitive to chlorophyll content at leaf and canopy (Hunt et al. 2011). Since this indice uses the bands in the visible region, chlorophyll content can be estimated with TGI on images acquired from UAVs equipped with an RGB camera.

$$TGI = Green - 0.39 \times Red - 0.61 \times Blue \quad (3)$$

## 3.2. Ensemble learning methods

### 3.2.1. Random forest (RF)

The RF algorithm, proposed by Breiman (2001), is one of the most popular decision tree based ensemble learning algorithms used for performing pixel-based image classification procedure due to its robust and efficient performance (Nitze et al., 2015; Fu et al., 2017). RF utilizes multiple decision trees in that each tree trained using bootstrapped samples of input dataset for constructing classification model. Majority voting rule is applied to make the final prediction and simple majority rule is applied for final prediction (Colkesen and Kavzoglu, 2017). Based on bootstrapping strategy, decision trees are trained using two thirds of input dataset and the remaining one-third of input dataset is utilized to evaluate the classification error (Tonbul et al., 2020). The results of each tree are aggregated, and final model output is composed. RF requires two main parameters to employ RF, such as the number of sample trees (*ntree*) and the number of variables suitable for splitting (*mtry*).

### 3.2.2. Extreme gradient boosting (XGBoost)

XGBoost, one of the advanced and effective tree-based algorithm presented by Chen and Guestrin (2016), has been used in various remote sensing applications due to its effective and fast performance (Zou et al., 2019; Abdi, 2020). It works based on essential of gradient boosting that construct multiple decision trees iteratively and transform weak learners to strong learners in each iteration (Sahin, 2020). The main difference of XGBoost than other tree-based algorithms, it uses the loss function to correct the error of weak learners of previous model in each iteration and employs regularization parameter to prevent overfitting to produce accurate classification model (Hamedianfar et al., 2020; Ustuner et al., 2020). XGBoost consists of several tuning parameters that should be defined by user-side. Seven parameters including eta, gamma, min_child_weight, subsample, colsample_bytree, max_depth, nround were optimized for XGBoost ensemble model in this study.

### 3.2.3. Light gradient boosting machines (LightGBM)

LightGBM, developed by Microsoft (2017), is one of the most preferred open-source and gradient boosting based method for regression and classification problems (Ma et al., 2018; Sun et al., 2020). It uses a histogram-based model that speeds up the training process and enables a more accurate model to be constructed (Al Daoud, 2019). The main difference between LightGBM and other gradient-based methods are that it utilizes gradient-based one-side sampling (GOSS) algorithms that divide training samples into smaller subsamples and leaf-wise growth strategy (Chen et al., 2019). LightGBM has several parameters and "boosting", "learning_rate", "num_leaves", "min_data", "sub_features", "feature_fraction", "bagging_fraction" and "max_depth" were tuned to construct classification model (Ke et al., 2017).

### 3.2.4. Categorical boosting (CatBoost)

CatBoost, novel gradient boosting method, was developed by Yandex (2018) for handle different datasets such as categorical features using random permutation technique and minimize overfitting problems (Pham et al., 2020). CatBoost consists of two main training steps. In the first step, training data is randomly divided into subsets and labels are transformed into integer. Categorical features are converted into numerical in the second step. The maximum depth of trees (depth), the control of training time (learning_rate), the number of trees in model (iteration), coefficient at the L2 regularization (l2_leaf_reg), the percentage of variables to utilize at each split selection (rms) and the controlling number of splits for numerical variables (border_count) were utilized for implementation of CatBoost ensemble classification model.

## 4. Results

In this study, the effect of VIs on pixel based LULC classification of RGB image acquired by UAV was investigated. To achieve this purpose, three VIs (i.e., GLI, RGBVI and TGI) were calculated using equation given in section 3.2 and stretched to 0-255 pixel values. In order to construct classification model and to evaluate accuracies of thematic maps, totally 30,000 pixels (i.e. 5,000 pixels for each LULC class) were selected as training and 6,000 pixels (i.e. 1,000 pixels for each LULC class) were selected as validation. Five datasets were created using RGB bands and different combination of VIs to evaluate classification results: Dataset-1 includes only RGB band, Dataset-2 consists of RGB bands and GLI, Dataset-3 consists of RGB bands and RGBVI, Dataset-4 consists of RGB bands and TGI and Dataset-5 corresponds to combination of RGB bands and all VIs considered. On the hand, parameters of each classifier should be determined by user side to obtain optimal classification models. Tuning parameters required for each ensemble methods were determined by grid search algorithm and estimated values were given in Table 2. Note that all classification processes and accuracy assessments were performed in R software. Additionally, the "randomForest", "xgboost", "lightgbm" and "catboost" packages were utilized for implementation of RF, XGBoost, LightGBM and CatBoost ensemble methods, respectively and "caret" package was utilized to calculate accuracy assessment measures.

**Table 2.** Optimal parameters of ensemble methods

| Method | Parameter | Value |
|---|---|---|
| RF | ntree | 380 |
| | mtry | 2 |
| XGBoost | eta | 0.3 |
| | gamma | 0 |
| | min_child_weight | 0.6 |
| | subsample | 0.8 |
| | colsample_bytree | 1 |
| | max_depth | 4 |
| | nround | 400 |
| LightGBM | boosting | goss |
| | learning_rate | 0.3 |
| | num_leaves | 20 |
| | min_data | 80 |
| | sub_features | 0.8 |
| | feature_fraction | 1 |
| | bagging_fraction | 1 |
| | max_depth | 4 |
| CatBoost | depth | 4 |
| | learning_rate | 0.3 |
| | iteration | 400 |
| | l2_leaf_reg | 0.7 |
| | rms | 0.95 |
| | border_count | 128 |

Accuracy assessment results of each Dataset were given in Table 3. As could be seen from the table, the highest OA values estimated for Dataset-5 as 91.2% (Kappa value of 0.89), 92.2% (Kappa value of 0.90), 92.0% (Kappa value of 0.90) and 92.4% (Kappa value of 0.91) by the use of RF, XGBoost, LightGBM and CatBoost, respectively. On the other hand, the lowest OA values were observed for Dataset-1 with all ensemble learning algorithms. Furthermore, the OA values of Dataset-4 calculated from all classifiers were very close to the OA values obtained with Dataset-5 (lower about 0.1%). Additionally, it was observed that calculated OA values increased by about 0.3% with the use of Dataset-2 compared to use of Dataset-3. When the classification results based on OA accuracy were evaluated it was seen that while the CatBoost showed quite similar performance to XGBoost and LightGBM, the highest OA value was obtained as 92.24% with the CatBoost algorithm. On the other hand, it has been observed that the classification performance of the RF algorithm is lower than that of the others for all datasets except for Dataset-1.

In order to evaluate and compare class-based accuracy performances, F-score values were also calculated, and derived statistics were given in Table 3. It can be seen that concrete, forest and parkour classes were classified with over 91% classification accuracy by all ensemble algorithms. Furthermore, the highest F-score values were estimated for parkour class, whereas the worst class-based accuracy calculated for soil class. The reason why the class-level accuracy of the soil class was lowest may be that various substances that were mixed into the soil and have similar spectral properties with other LULC classes could be easily distinguished in the images obtained with the UAV. Moreover, with the classification of the RGB bands with all calculated indices (Dataset-5), the F-score value of soil class produced by all classifiers increased up to 4% compared to results of Dataset-1. Furthermore, the accuracies of concrete class estimated by XGBoost, LightGBM and CatBoost for Dataset-4 were significantly higher than result of RF (about 3%).

**Table 3.** Classification results of each dataset

| Method | LULC Class | F-scores D-1 | D-2 | D-3 | D-4 | D-5 |
|---|---|---|---|---|---|---|
| RF | Concrete | 91.3 | 91.8 | 92.4 | 92.4 | 94.6 |
| | Forest | 97.5 | 97.0 | 96.9 | 97.2 | 96.7 |
| | Parkour | 98.5 | 99.4 | 99.5 | 99.7 | 99.2 |
| | Shadow | 89.2 | 90.4 | 90.0 | 90.5 | 89.9 |
| | Soil | 79.5 | 81.2 | 79.5 | 80.0 | 80.0 |
| | Tile roof | 84.5 | 85.8 | 85.9 | 87.2 | 87.3 |
| | OA | 90.0 | 90.8 | 90.6 | 91.1 | 91.2 |
| | Kappa | 0.88 | 0.89 | 0.89 | 0.89 | 0.89 |
| XGBoost | Concrete | 91.6 | 92.8 | 93.4 | 95.5 | 95.8 |
| | Forest | 97.4 | 96.3 | 96.1 | 97.9 | 97.8 |
| | Parkour | 98.0 | 98.7 | 98.4 | 98.7 | 99.4 |
| | Shadow | 88.7 | 91.1 | 91.1 | 89.8 | 91.1 |
| | Soil | 79.7 | 82.2 | 80.2 | 81.3 | 81.2 |
| | Tile roof | 84.4 | 86.6 | 86.7 | 88.5 | 88.2 |
| | OA | 89.9 | 91.2 | 90.9 | 92.0 | 92.2 |
| | Kappa | 0.88 | 0.89 | 0.89 | 0.90 | 0.90 |
| LightGBM | Concrete | 92.9 | 92.5 | 93.8 | 95.3 | 95.7 |
| | Forest | 97.1 | 96.6 | 96.6 | 97.6 | 97.1 |
| | Parkour | 97.1 | 98.8 | 98.8 | 98.6 | 98.8 |
| | Shadow | 88.4 | 90.8 | 91.4 | 90.2 | 91.2 |
| | Soil | 79.2 | 81.4 | 81.2 | 81.9 | 81.2 |
| | Tile roof | 85.1 | 86.2 | 86.7 | 88.3 | 88.2 |
| | OA | 89.8 | 91.0 | 91.3 | 91.9 | 92.0 |
| | Kappa | 0.88 | 0.90 | 0.90 | 0.90 | 0.90 |
| CatBoost | Concrete | 92.2 | 92.6 | 95.5 | 95.3 | 95.8 |
| | Forest | 97.1 | 97.7 | 96.5 | 97.8 | 97.7 |
| | Parkour | 97.9 | 99.7 | 99.1 | 99.1 | 99.6 |
| | Shadow | 89.5 | 90.7 | 90.4 | 90.7 | 91.4 |
| | Soil | 80.1 | 82.1 | 81.3 | 82.5 | 81.2 |
| | Tile roof | 85.6 | 86.8 | 88.4 | 88.9 | 88.3 |
| | OA | 90.4 | 91.5 | 91.8 | 92.3 | 92.4 |
| | Kappa | 0.89 | 0.90 | 0.90 | 0.91 | 0.91 |

To visual comparison of datasets, thematic maps were produced by RF and CatBoost classifiers which yield the lowest and highest OA values and presented in Figure 2. Determined misclassification error on the thematic maps are highlighted with a dashed white circle. According to visual analysis, thematic maps produced by CatBoost were smoother than those of RF. On the other hand, main classification errors were occurred among concrete, soil, shadow and tile roof. It was observed that both ensemble methods were insufficient in distinguishing soil, shadow and concrete classes. This visual result is consistent with the F-score values of the soil class. As can be seen from marked areas, CatBoost outperformed to RF in assigning the pixels corresponding to the concrete class to the correct land cover class. Additionally, the noise generated in the concrete class was reduced in the thematic map produced by RF using Dataset-5 compared to other thematic maps by RF.

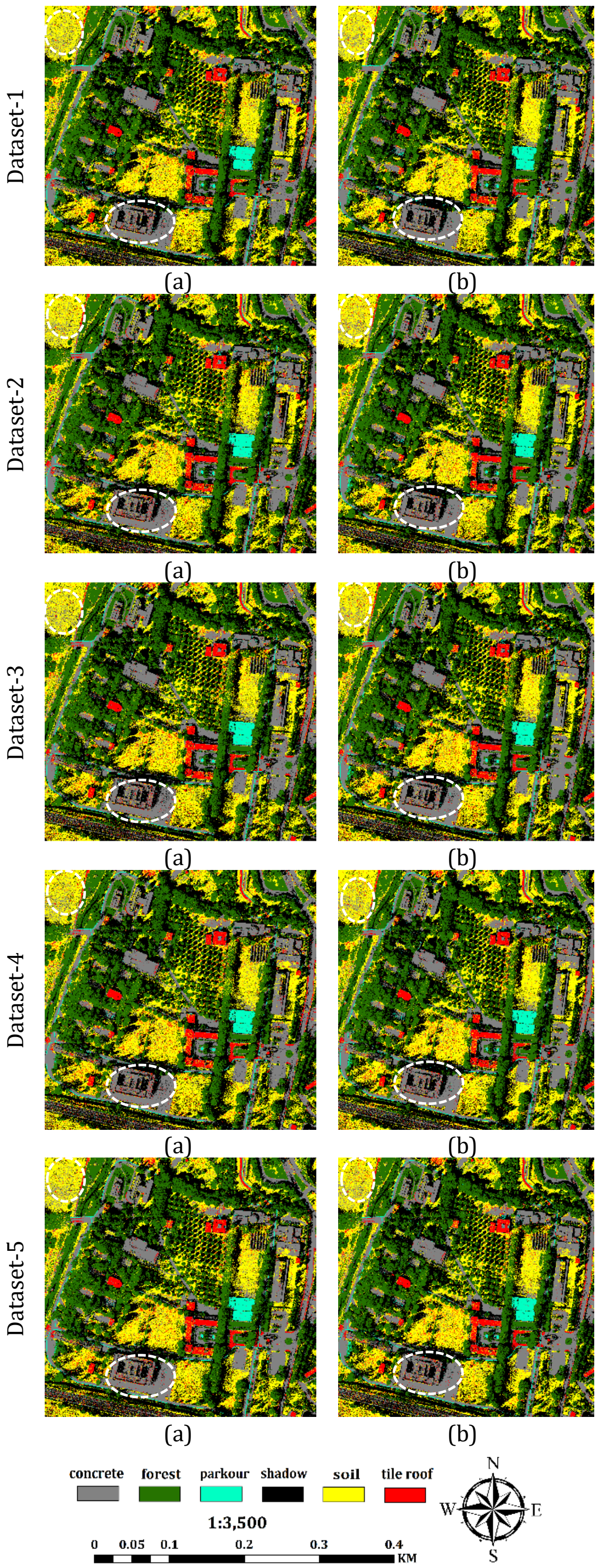


**Figure 2.** Thematic maps of each dataset produced by (a) RF, (b) CatBoost.

## 4. Discussion and conclusions

In recent years, there has been an increasing interest in the production of thematic maps with UAV images using ensemble learning algorithms due to their effective classification performance. VIs used to highlight the features of the Earth's provide a great advantage in increasing the spectral information in the pixel-based classification of RGB images. In this context, the effects of widely used three VIs (i.e. GLI, RGBVI and TGI) on the classification of UAV image having three spectral bands were investigated. For this purpose, five datasets containing different combination of VIs and UAV image were created and each dataset was classified with RF, XGBoost, LightGBM and CatBoost.

The following conclusions can be made by analyzing the classification results obtained. OA values obtained by the classification of UAV image with VIs (Dataset-5) increased by 1% with the use of RF and by 2% with other remaining methods compared to results of visible spectral bands only (Dataset-1). This could be probably result of the increase in spectral information by means of vegetation indices usage. Kerkech et al. (2018), Wan et al. (2018) and Lu et al. (2021) analyzed the performance of several VIs derived from RGB drone images. They reported that while the highest classification and regression accuracies were computed in the processing of the RGB image with all evaluated vegetation indices, the accuracy decreased as the spectral information decreased. On the other hand, the OA values of Dataset-4 (combination of RGB bands and TGI) generated by all the algorithms are about 0.1% less than the classification results of Dataset-5. Additionally, all ensemble learning methods yielded higher classification results in the use of UAV image with TGI compared to datasets consisting of aggregation of RGB band with other indices (Dataset-2 and Dataset-3). These results clearly showed that TGI was found to be the most useful indices to identification of LULC classes in classifying three-band UAV images for considered dataset used in this study. Fuentes-Peailillo et al. (2018) analyzed the various RGB-based vegetation indexes for distinguishing soil and vegetation areas and they found that TGI index showed superior performance than other VIs. Starý et al. (2020) conducted comparative study using seven RGB-based VIs including GLI, RGBVI and TGI indexes for estimating hops plants in hop gardens and TGI outperformed to others in their study. Hindersah et al. (2018) also found similar results with our study. Moreover, CatBoost, relatively new ensemble learning algorithm, showed superior classification performance in separation of LULC classes compared to other algorithms. The implementation of CatBoost for classification and regression problems of remote sensing problems in the literature is very limited. In addition, pixel-based classification of UAV images has not been made with this algorithm until now. However, it was verified by Samat et al. (2020), Ha et al. (2021) and Pham et al. (2021) that CatBoost have effective and superior classification and regression performance compared to other bagging, boosting and other classifiers (i.e., RF, XGBoost, SVM). Our findings also contribute their studies. Different vegetation indices can be evaluated with various robust classifiers (e.g., support vector machines, canonical corelation forest, rotation forest) in order to better analyse the effect of VIs on the classification of the RGB image. In addition, further studies are required to evaluate the effectiveness of the use of RGB derived vegetation indices on object-based classification accuracy.

**Acknowledgement**

This article is presented in "2nd Intercontinental Geoinformation Days" 2021 and selected for publication in Mersin Photogrammetry Journal.

**Author contributions**

**Muhammed Yusuf Öztürk:** Literature review, Field study, Modelling, classification, Writing **İsmail Çölkesen:** Modelling, classification, Writing-editing.

**Conflicts of interest**

The authors declare no conflicts of interest.

**References**

Abdi A M (2020). Land cover and land use classification performance of machine learning algorithms in a boreal landscape using Sentinel-2 data. *GIScience & Remote Sensing*, *57*(1), 1–20. https://doi.org/10.1080/15481603.2019.1650447

Al Daoud E (2019). Comparison between XGBoost, LightGBM and CatBoost Using a Home Credit Dataset. *International Journal of Computer and Information Engineering*, *13*(1), 6–10.

Breiman L (2001). Random Forests. In *Machine Learning* (pp. 5–32). Chapman and Hall/CRC. https://doi.org/10.1023/A:1010933404324

Chen Tianqi & Guestrin C (2016). XGBoost. *Proceedings of the 22nd ACM SIGKDD International Conference on Knowledge Discovery and Data Mining*, *13-17-Augu*, 785–794. https://doi.org/10.1145/2939672.2939785

Chen Tingting, Xu J, Ying H, Chen X, Feng R, Fang X, Gao H & Wu J (2019). Prediction of Extubation Failure for Intensive Care Unit Patients Using Light Gradient Boosting Machine. *IEEE Access*, *7*, 150960–150968. https://doi.org/10.1109/ACCESS.2019.2946980

Colkesen I & Ertekin O H (2020). Performance Analysis of Advanced Decision Forest Algorithms in Hyperspectral Image Classification. *Photogrammetric Engineering & Remote Sensing*, *86*(9), 571–580. https://doi.org/10.14358/PERS.86.9.571

Colkesen I & Kavzoglu T (2017). The use of logistic model tree (LMT) for pixel- and object-based classifications using high-resolution WorldView-2 imagery. *Geocarto International*, *32*(1), 71–86. https://doi.org/10.1080/10106049.2015.1128486

Fu B, Wang Y, Campbell A, Li Y, Zhang B, Yin S, Xing Z & Jin X (2017). Comparison of object-based and pixel-based Random Forest algorithm for wetland vegetation mapping using high spatial resolution GF-1 and SAR data. *Ecological Indicators*, *73*, 105–117. https://doi.org/10.1016/j.ecolind.2016.09.029

Fuentes-Peailillo F, Ortega-Farias S, Rivera M, Bardeen M & Moreno M (2018). Comparison of vegetation indices acquired from RGB and Multispectral sensors placed on UAV. *2018 IEEE International Conference on Automation/XXIII Congress of the Chilean Association of Automatic Control (ICA-ACCA)*, 1–6. https://doi.org/10.1109/ICA-ACCA.2018.8609861

Goldblatt R, Stuhlmacher M F, Tellman B, Clinton N, Hanson G, Georgescu M, Wang C, Serrano-Candela F, Khandelwal A K, Cheng W H & Balling R C (2018). Using Landsat and nighttime lights for supervised pixel-based image classification of urban land cover. *Remote Sensing of Environment*, *205*(December 2017), 253–275. https://doi.org/10.1016/j.rse.2017.11.026

Ha N T, Manley-Harris M, Pham T D & Hawes I (2021). Detecting multi-decadal changes in seagrass cover in tauranga harbour, new zealand, using landsat imagery and boosting ensemble classification techniques. *ISPRS International Journal of Geo-Information*, *10*(6). https://doi.org/10.3390/ijgi10060371

Hamedianfar A, Gibril M B A, Hosseinpoor M & Pellikka P K E (2020). Synergistic use of particle swarm optimization, artificial neural network, and extreme gradient boosting algorithms for urban LULC mapping from WorldView-3 images. *Geocarto International*, *0*(0), 1–19. https://doi.org/10.1080/10106049.2020.1737974

Hindersah R, Handyman Z, Indriani F N, Suryatmana P & Nurlaeny N (2018). JOURNAL OF DEGRADED AND MINING LANDS MANAGEMENT Azotobacter population, soil nitrogen and groundnut growth in mercury-contaminated tailing inoculated with Azotobacter. *J. Degrade. Min. Land Manage*, *5*(53), 2502–2458. https://doi.org/10.15243/jdmlm

Hunt E R, Daughtry C S T, Eitel J U H & Long D S (2011). Remote Sensing Leaf Chlorophyll Content Using a Visible Band Index. *Agronomy Journal*, *103*(4), 1090–1099. https://doi.org/10.2134/agronj2010.0395

Huth J, Kuenzer C, Wehrmann T, Gebhardt S, Tuan V Q & Dech S (2012). Land cover and land use classification with TWOPAC: Towards automated processing for pixel- and object-based image classification. *Remote Sensing*, *4*(9), 2530–2553. https://doi.org/10.3390/rs4092530

Jang G, Kim J, Yu J, Kim H, Kim Y, Kim D, Kim K, Lee C W & Chung Y S (2020). Remote sensing Review : Cost-E ff ective Unmanned Aerial Vehicle ( UAV ) Platform for Field Plant Breeding Application. *Remote Sensing*, *12*(6), 998.

Ke G, Meng Q, Finley T, Wang T, Chen W, Ma W, Ye Q & Liu T Y (2017). LightGBM: A highly efficient gradient boosting decision tree. *Advances in Neural Information Processing Systems*, *2017-Decem*(Nips), 3147–3155.

Kerkech M, Hafiane A & Canals R (2018). Deep leaning approach with colorimetric spaces and vegetation indices for vine diseases detection in UAV images. *Computers and Electronics in Agriculture*, *155*(October), 237–243. https://doi.org/10.1016/j.compag.2018.10.006

Lu J, Cheng D, Geng C, Zhang Z, Xiang Y & Hu T (2021). Combining plant height, canopy coverage and vegetation index from UAV-based RGB images to estimate leaf nitrogen concentration of summer maize. *Biosystems Engineering*, *202*, 42–54.

https://doi.org/10.1016/j.biosystemseng.2020.11.010

Ma X, Sha J, Wang D, Yu Y, Yang Q & Niu X (2018). Study on a prediction of P2P network loan default based on the machine learning LightGBM and XGboost algorithms according to different high dimensional data cleaning. *Electronic Commerce Research and Applications*, *31*, 24–39. https://doi.org/10.1016/j.elerap.2018.08.002

Nitze I, Barrett B & Cawkwell F (2015). Temporal optimisation of image acquisition for land cover classification with Random Forest and MODIS time-series. *International Journal of Applied Earth Observation and Geoinformation*, *34*(1), 136–146. https://doi.org/10.1016/j.jag.2014.08.001

Pham T D, Yokoya N, Nguyen T T T, Le N N, Ha N T, Xia J, Takeuchi W & Pham T D (2020). Improvement of Mangrove Soil Carbon Stocks Estimation in North Vietnam Using Sentinel-2 Data and Machine Learning Approach. *GIScience & Remote Sensing*, 1–20. https://doi.org/10.1080/15481603.2020.1857623

Pham T D, Yokoya N, Nguyen T T T, Le N N, Ha N T, Xia J, Takeuchi W & Pham T D (2021). Improvement of Mangrove Soil Carbon Stocks Estimation in North Vietnam Using Sentinel-2 Data and Machine Learning Approach. *GIScience & Remote Sensing*, *58*(1), 68–87. https://doi.org/10.1080/15481603.2020.1857623

Sagi O & Rokach L (2018). Ensemble learning: A survey. *Wiley Interdisciplinary Reviews: Data Mining and Knowledge Discovery*, *8*(4), 1–18. https://doi.org/10.1002/widm.1249

Sahin E K (2020). Comparative analysis of gradient boosting algorithms for landslide susceptibility mapping. *Geocarto International*, *0*(0), 1–25. https://doi.org/10.1080/10106049.2020.1831623

Samat A, Li E, Du P, Liu S, Miao Z & Zhang W (2020). CatBoost for RS Image Classification With Pseudo Label Support From Neighbor Patches-Based Clustering. *IEEE Geoscience and Remote Sensing Letters*, 1–5. https://doi.org/10.1109/LGRS.2020.3038771

Shi J, Shao T, Liu X, Zhang X, Zhang Z & Lei Y (2021). Evolutionary Multitask Ensemble Learning Model for Hyperspectral Image Classification. *IEEE Journal of Selected Topics in Applied Earth Observations and Remote Sensing*, *14*, 936–950. https://doi.org/10.1109/JSTARS.2020.3037353

Starý K, Jelínek Z, Kumhálova J, Chyba J & Balážová K (2020). Comparing RGB-based vegetation indices from uav imageries to estimate hops canopy area. *Agronomy Research*, *18*(4), 2592–2601. https://doi.org/10.15159/AR.20.169

Sumesh K C, Ninsawat S & Som-ard J (2021). Integration of RGB-based vegetation index, crop surface model and object-based image analysis approach for sugarcane yield estimation using unmanned aerial vehicle. *Computers and Electronics in Agriculture*, *180*(July 2020), 105903. https://doi.org/10.1016/j.compag.2020.105903

Sun X, Liu M & Sima Z (2020). A novel cryptocurrency price trend forecasting model based on LightGBM. *Finance Research Letters*, *32*(November 2018), 101084. https://doi.org/10.1016/j.frl.2018.12.032

Tehrany M S, Pradhan B & Jebuv M N (2014). A comparative assessment between object and pixel-based classification approaches for land use/land cover mapping using SPOT 5 imagery. *Geocarto International*, *29*(4), 351–369. https://doi.org/10.1080/10106049.2013.768300

Tonbul H, Colkesen I & Kavzoglu T (2020). Classification of poplar trees with object-based ensemble learning algorithms using Sentinel-2A imagery. *Journal of Geodetic Science*, *10*(1), 14–22. https://doi.org/10.1515/jogs-2020-0003

Ustuner M, Abdikan S, Bilgin G & Balik Sanli F (2020). Hafif Gradyan Artırma Makineleri ile Tarımsal Ürünlerin Sınıflandırılması. *Türk Uzaktan Algılama ve CBS Dergisi*, *1*(2), 97–105.

Wan L, Li Y, Cen H, Zhu J, Yin W, Wu W, Zhu H, Sun D, Zhou W & He Y (2018). Combining UAV-Based Vegetation Indices and Image Classification to Estimate Flower Number in Oilseed Rape. *Remote Sensing*, *10*(9), 1484. https://doi.org/10.3390/rs10091484

Xue J & Su B (2017). Significant Remote Sensing Vegetation Indices: A Review of Developments and Applications. *Journal of Sensors*, *2017*, 1–17. https://doi.org/10.1155/2017/1353691

Yao H & Qin R (2019). *Unmanned Aerial Vehicle for Remote Sensing Applications — A Review*. *11*(12), 1443.

Zhiwei Y, Juan Y, Xu Z & Zhengbing H (2016). Remote Sensing Textual Image Classification based on Ensemble Learning. *International Journal of Image, Graphics and Signal Processing*, *8*(12), 21–29. https://doi.org/10.5815/ijigsp.2016.12.03

Zou X, Liang A, Wu B, Su J, Zheng R & Li J (2019). UAV-based high-throughput approach for fast growing Cunninghamia lanceolata (Lamb.) cultivar screening by machine learning. *Forests*, *10*(9). https://doi.org/10.3390/f10090815

*Mersin Photogrammetry Journal – 2021; 3(2); 48-52*

**Mersin Photogrammetry Journal**

https://dergipark.org.tr/en/pub/mephoj

**e-ISSN 2687-654X**

# Three-dimensional modeling and drawings of stone column motifs in Harran Ruins

**Yunus Kaya*[1], Halil İbrahim Şenol[1], Nizar Polat[1]**

[1]*Harran University, Faculty of Engineering, Department of Geomatics Engineering, Şanlıurfa, Turkey*

**Keywords**
Archaeology
Photogrammetry
3D Model
Harran

**ABSTRACT**

The preservation, documentation, and transmission of archaeological artifacts, which are also defined as heritage, can be accepted as the common responsibility of humanity. To document the cultural heritage, the status of historical artifacts should be known. The photogrammetry technique has been commonly used in the documentation of cultural heritage in parallel with the technological developments recently. In addition to producing map and topographic products, generating three-dimensional models from two-dimensional photographs has brought the photogrammetry method to an important position. For this reason, contributions are made to different disciplines such as archeology. Digital documentation of archaeological artifacts provides serious advantages. In this study, some of the destroyed stone column samples found in Harran Ruins were modeled by using Structure from Motion (SfM) method. At the end of the study the point clouds, digital surface models, orthoimages and stone column motifs were obtained.

## 1. Introduction

Historical artifacts are cultural heritages that host hundreds of years of information, and this information should be handed down to the next generations. While these historical heritages reflect the lifestyle and sense of aesthetics of the ancient civilization; they have changed over time due to natural and artificial effects such as wars and earthquakes. Documenting and preserving the natural texture of historical artifacts without damage is an indispensable factor for handing them down to the next generations. It is a fact that cultural heritage is damaged not only in our country but also in many parts of the world. For this reason, the documentation of cultural heritage is among the hot topics all over the world.

Documentation of archaeological artifacts and cultural heritage is a complex process (Kulur and Yılmaztürk, 2005; Ulvi et al., 2020). Documentation of archaeological artifacts consists of the study, process, storage, and presentation steps necessary to determine the current state (shape and location) of the structure in three-dimensional (3D) (Georgopoulos and Ioannidis, 2004). There are several techniques for documenting cultural heritage (Bohler and Heinz, 1999; Şanlıoğlu et al., 2013). Photogrammetry (Kaya et al., 2021; Ulukavak et al., 2019; Polat et al., 2020) and scanning methods (Senol et al., 2017) are at the forefront of these very important and necessary techniques (Bohler and Heinz, 1999; Scherer, 2002; Şenol et al., 2020). At this point, it is a great advantage that photogrammetry can provide reliable information in a short time (Yakar et al., 2011; Şasi and Yakar, 2018).

Today, with the development of photogrammetry and computer vision disciplines, image-based modeling techniques have become a serious competitor to laser scanning (Remondino et al., 2011). Some notable advantages of image-based modeling are it is low cost and contains color information, calibrated or uncalibrated cameras are acceptable (Colomina et al., 2008) and can produce a denser cloud of points than a laser scanner. At this point, unlike classical photogrammetry, the motion-based structural detection (Structure from Motion -SfM) approach is widely used (Polat et al., 2020). SfM operates under the same basic conditions as Photogrammetry. Overlapping images are used to obtain the 3D structure of the object of interest. Many commercial software such as Agisoft

* **Corresponding Author**

* yunuskaya@harran.edu.tr) ORCID ID 0000-0003-2319-4998
(hsenol@harran.edu.tr) ORCID ID 0000-0003-0235-5764
(nizarpolat@harran.edu.tr) ORCID ID 0000-0002-6061-7796

**Cite this article**

Kaya Y, Şenol H İ & Polat N (2021). Three-dimensional modeling and drawings of stone column motifs in Harran Ruins. *Mersin Photogrammetry Journal, 3(2), 48-52*

**Research Article / DOI: 10.53093/mephoj.1012937**

**Received: 21/10/2021; Accepted: 22/11/2021**

Photoscan are also widely used for 3D modeling. In general, it allows to produce many products such as matching photos, producing sparse and dense point clouds, three-dimensional model, digital elevation model and orthophoto. Image processing steps can take serious time. For this reason, the use of high-performance computers is especially recommended to produce a full-performance 3D model (Siebert and Teizer, 2014). In this study, three-dimensional models of some of the figures found in the historical Harran Archaeological Site were created digitally by the SfM method and three selected stone column motifs were drawn.

## 2. Method

### 2.1. Study area

The study was carried out at the excavation site in İçkale, Harran Ruins in the Harran district of Şanlıurfa (Figure 1). The wall structures and infrastructure of the Harran region, which is one of the oldest settlements of human civilization, have been built, repaired, enlarged or reduced in a very long time. The Old Harran region, which dates back to 5000 BC, is an important city in Upper Mesopotamia. There are many historical artifacts from different civilizations in the region. One of the most important of these is the Harran castle. The parts where active excavation and repair have been completed are open to touristic visits. Archaeological studies have been carried out on the relevant region at different times. Today, with the support of the Ministry of Culture and Tourism, the Turkish Historical Society, Harran University and local support, Prof. Dr. Mehmet ÖNAL and his archeology team carry out archaeological excavations in the Harran Ruins. During the studies carried out in İçkale, the Kale Bath (Önal, 2019; Önal, 2020), the South-East Gate and the rectangular tower and the second defense system in the west of the castle were unearthed. Excavations continue on the remains of the castle bridge. In the study, some of the destroyed stone column motifs samples found in the excavation area of Harran Ruins were modeled in three dimensions and drawn.

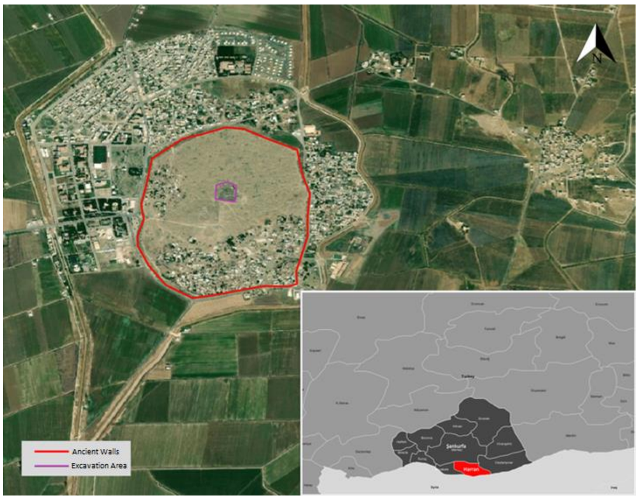


**Figure 1.** The ancient city of Harran, the excavation site and the location of the town of Harran

### 2.2. Equipment

Embossed figures in the archaeological area have been documented by the SfM. Overlay photographs are required to cover the entire object so that the documentation process can be done precisely. Canon EOS 2000D model DSLR camera was used for this process in the study. Information about the digital camera used is given in Table 1.

**Table 1.** Technical specifications of the camera used

| Feature | Value |
|---|---|
| Megapixel | 24.1 |
| Maximum resolution | 6000 x 4000 |
| Weight | 475 g |
| Size | 129 x 101.3 x 77.6 mm |
| Sensor size | 22.3 x 14.9 mm |

### 2.3. Application

In the study, dense point cloud and 3D model of three different models were produced with photographs taken from the ground. Terrestrial photogrammetry, which is a useful method for structures no larger than human height, can convert photos taken with simple digital handheld cameras into high-precision 3D models. The stones with figures, which are the subject of the study, are modeled in 3D with the SfM method, which is widely used in the world. Although the SfM approach was developed by the computer vision community to achieve an automatic image matching algorithm, it works under the same basic conditions as Stereoscopic Photogrammetry (Tanskanen et al., 2013; Snavely, 2009; Westoby et al., 2012; Micheletti et al., 2015). Overlapping images are used to obtain the 3D form of the object of interest (Yakar et al. 2005). However, there is a fundamental difference between traditional Photogrammetry and SfM. In traditional Photogrammetry, the 3D position of cameras or the 3D position of ground control points (GCP) must be known to determine the 3D position of points in an image (Yakar et al. 2010). In contrast, SfM automatically determines the geometric parameters (orientation, internal and external parameters) without any known predefined set of GCPs. Instead, these parameters are resolved simultaneously using a highly overlapping image set with the same features automatically mapped (Snavely, 2009). Then, the iterative, non-linear least squares minimization process traces the matching features from image to image, estimating camera positions and object coordinates. Compared to traditional photogrammetry, the camera positions determined are in the image space, meaning there is no scale and no orientation when considering the object area. This is solved by 3D similarity transformation using a small number of ground control points in areas such as map production (Westoby et al., 2012). In object modeling, it is often sufficient to specify a scale. To get a useful 3D geometry of the object, the images must fully cover the object (Yakar et al. 2015). In order to fulfill this condition, it is necessary for the camera to view the object from every angle.

## 3. Results

In this study, reliefs on 3 historical stones with figures on them were extracted by relief method that found in the archaeological excavation area of the historical Harran Ruins were discussed. The inscription fragments we obtained after the excavation were broken over time and underwent physical changes (Figure 2). In order to document the stones digitally, 3D modeling was carried out with the photogrammetry method. For this purpose, three different stones that were found during the excavations and waiting to be classified were examined as examples (Figure 2).

**Figure 2.** Images of selected stone column motifs

For the three pieces of stones, 38, 52 and 33 photographs were taken locally, respectively. In order to model the figures exactly, photographs of the objects were taken from all angles as much as possible. As the stones were lined up at the bottom of the castle wall, the desired number of photographs could not be obtained by the wall (Figure 3).

The number of 3D model triangles also increases and decreases proportionally to the number of point clouds. At least over five million 3D points are produced, modeled with high density. 3D models were obtained from the produced point clouds and photorealistic models were obtained by covering these models with real color texture. To visualize the figures in the models more clearly, only the surface of the models with the inscriptions was taken and the height model of the surface was obtained (Figure 3). Thanks to the height model produced, the legibility of the letters is increased as the embossments formed by the letters are colored differently from the ground. Drawings were made to increase the intelligibility of the patterns. The patterns on the stones were drawn by hand.

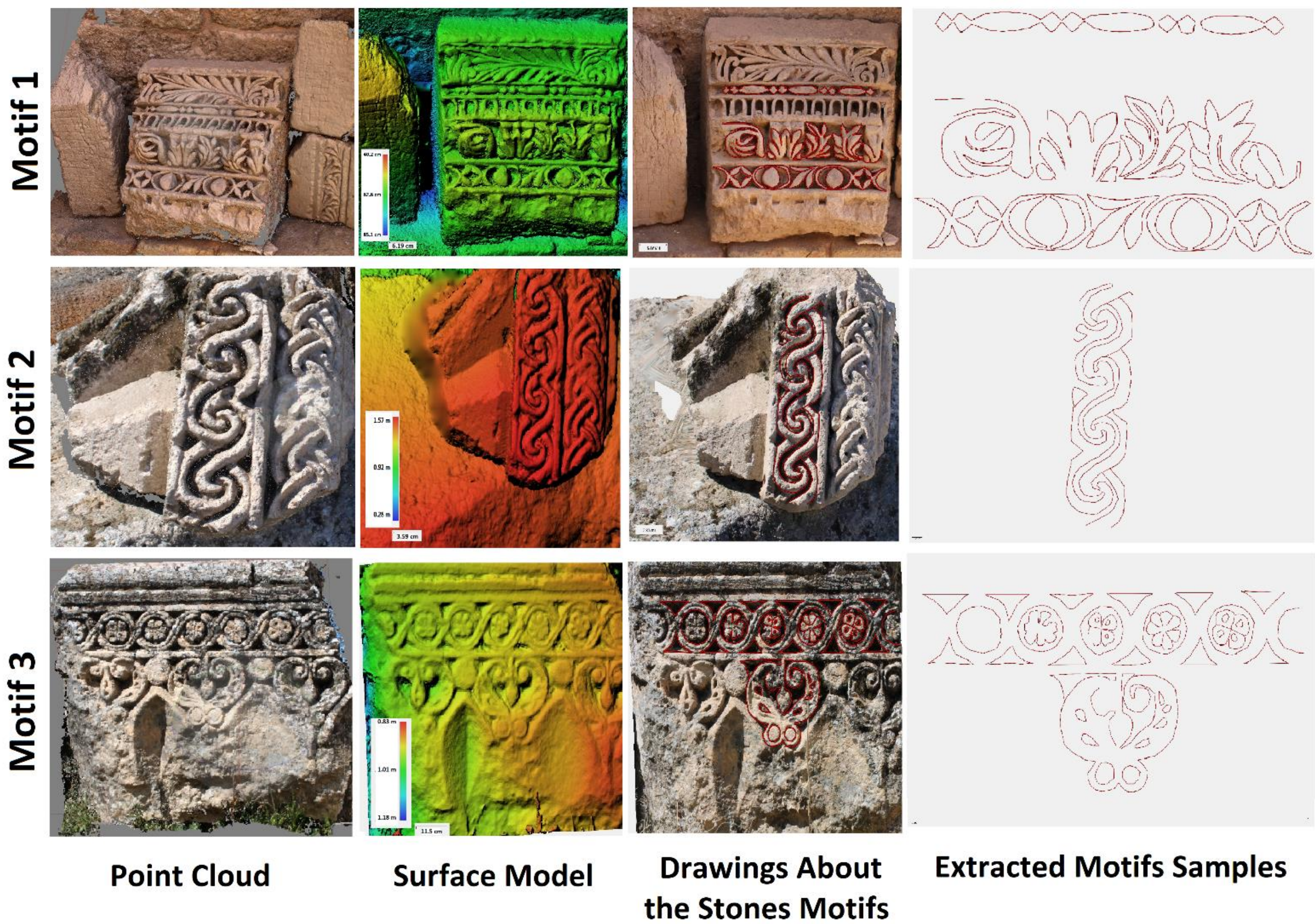


**Figure 3.** Point Cloud, Surface Model, Drawings About the Stone Motifs and Extracted Motifs

## 4. Results

It is very important in terms of protecting and documenting our cultural heritage, which should be transferred to future generations. In this context, the samples selected from the stones found in the Harran archaeological excavation area were modeled by the photogrammetric method. The digital records obtained with the three-dimensional modeling carried out contribute to the creation of digital archives of the works. In addition to these, the three-dimensional models obtained can also be used in restoration and restitution studies. Photogrammetric products such as the resulting three-dimensional model and point cloud are also in a position to meet the needs of studies in different disciplines. In the study, three different pieces of stone figures were selected, photographed and processed photogrammetrically. As a result, a three-dimensional model and a digital surface model of the stone surface were obtained. The figures that can be seen from the digital surface model were read and recorded. Figured stones damaged by environmental factors such as abrasion, breakage and algae are difficult to seen and perceive with the naked eye. Thanks to the models obtained in 3D by the photogrammetric method, perception and reading convenience are achieved. As a result, the photogrammetric approach offers serious contributions in terms of digital documentation, three-dimensional modeling and drawing of stone column motifs. In future studies, all stone motif, patterns, and ornaments found in the Harran ruins are planned to be modeled and documented digitally.

**Author contributions**

**Yunus Kaya**: Visualization, Investigation, Writing-Original draft preparation. **Halil İbrahim Şenol**: Visualization, Investigation, Writing-Reviewing, and Editing; **Nizar Polat**: Data curation, Conceptualization, Software, Validation.

**Conflicts of interest**

The authors declare no conflicts of interest.

**References**


Bohler W & Heinz G (1999). Documentation, surveying, photogrammetry. XVII CIPA Symposium. Recife, Olinda.

Colomina I, Blázquez M, Molina P, Parés M E, Wis M (2008). Towards a New Paradigm for High-Resolution Low-Cost Photogrammetry and Remote Sensing. IAPRS&SIS, 1201-1206.

Georgopoulos A & Ioannidis G (2004). Photogrammetric and Surveying Methods for the Geometric Recording of Archaeological Monuments, Archaeological Surveys. FIG Working Week 2004, May 22– 27, 2004, Athens, Greece.

Kaya Y, Yiğit A Y, Ulvi A & Yakar M (2021). Arkeolojik Alanların Dokümantasyonununda Fotogrametrik Tekniklerinin Doğruluklarının Karşılaştırmalı Analizi: Konya Yunuslar Örneği. Harita Dergisi, 165: 57-72.

Kulur S & Yilmazturk F (2005). 3D Reconstruction of Small Historical Objects to Exhibit in Virtual Museum by Means of Digital Photogrammetry. CIPA XX. International Symposium, International Cooperation to Save the World`s Cultural Heritage, 26 Sep.-01 Oct., Torino, Italy.

Micheletti N, Chandler J H & Lane S N (2015). Investigating the geomorphological potential of freely available and accessible structure-from-motion photogrammetry using a smartphone. Earth Surface Processes and Landforms, 40 (4): 473-486.

Önal M (2019). Harran 2017 Yılı Çalışmaları, 40. Kazı Sonuçları Toplantısı. 2. Cilt, Ankara, 632- 650.

Önal M (2020). Harran 2018 Yılı Çalışmaları, 41. Kazı Sonuçları Toplantısı 3. Cilt. Ankara, 157- 180.

Polat N, Önal M, Ernst F B, Şenol H İ, Memduhoğlu A, Mutlu S, Mutlu S İ, Budan M A, Turgut M & Kara H (2020). Harran Ören Yeri Arkeolojik Kazı Alanınından Çıkarılan Bazı Küçük Arkeolojik Buluntuların Fotogrametrik Olarak 3B Modellenmesi. Türkiye Fotogrametri Dergisi, 2 (2), 55-59.

Remondino F, Barazzetti L, Nex F, Scaioni M & Sarazzi D (2011). UAV Photogrammetry for Mapping and 3D Modeling Current Status and Future Perspectives. ISPRS ICWG I/V UAV-g Conference, Zurich, Switzerland.

Scherer M (2002). About the Synthesis of Different Methods in Surveying. XVIII International Symposium of CIPA, Potsdam, Germany.

Senol H I, Erdogan S, Onal M, Ulukavak M, Memduhoglu A, Mutlu S, Ernst F B & Yilmaz M (2017). 3D Modeling of a Bazaar in Ancient Harran City Using Laser Scanning Technique. International Archives of the Photogrammetry, Remote Sensing & Spatial Information Sciences, 42.

Siebert S & Teizer J (2014). Mobile 3D Mapping for Surveying Earthwork Projects Using an Unmanned Aerial Vehicle (UAV) System. Autom. Constr., 41: 1-14.

Snavely N K (2009). Scene Reconstruction and Visualization From Internet Photo Collections. Doctoral Thesis, University of Washington.

Şanlıoğlu İ, Zeybek M & Karauğuz G (2013). Photogrammetric Survey and 3D Modeling of Ivriz Rock Relief in Late Hittite Era. Mediterranean Archaeology and Archaeometry, 13 (2): 147-157.

Şasi A & Yakar M (2018). Photogrammetric Modelling of Hasbey Dar'ülhuffaz (Masjid) Using an Unmanned Aerial Vehicle. International Journal of Engineering and Geosciences, 3 (1), 6-11.

Şenol H İ, Memduhoglu A & Ulukavak M (2020). Multi Instrumental Documentation and 3D Modelling of an Archaeological Site: a Case Study in Kizilkoyun Necropolis Area. Dicle Üniversitesi Mühendislik Fakültesi Mühendislik Dergisi, 11 (3): 1241-1250.

Tanskanen P, Kolev K, Meier L, Camposeco F, Saurer O & Pollefeys M (2013). Live Metric 3D Reconstruction on Mobile Phones. in: 2013 IEEE Int. Conf. Comput. Vis., IEEE, 65-72.

Ulukavak M, Memduhoğlu A, Şenol H İ & Polat N (2019). Excavation Monitoring With UAV in Şanlıurfa Castle Archaeological Site. Mersin Photogrammetry Journal, 1 (1): 23-26.

Ulvi A, Yakar M, Yiğit A Y & Kaya Y (2020). İHA ve Yersel Fotogrametrik Teknikler Kullanarak Aksaray Kızıl Kilise’nin 3 Boyutlu Nokta Bulutu ve Modelinin Üretilmesi. Geomatik Dergisi, 5 (1), 22-30.

Westoby M J, Brasington J, Glasser N F, Hambrey M J & Reynolds J M (2012). Structure-fromMotion'photogrammetry: A Low-Cost, Effective Tool for Geoscience Applications. Geomorphology, 179: 300-314.

Yakar M, Yıldız F & Yılmaz H M (2005). Tarihi ve Kültürel Miraslarin Belgelenmesinde Jeodezi Fotogrametri Mühendislerinin Rolü. TMMOB Harita ve Kadastro Mühendisleri Odası, 10.

Yakar M, Yılmaz H M & Mutluoğlu Ö (2010). Comparative evaluation of excavation volume by TLS and total topographic station based methods. Lasers in Eng,19, 331-345.

Yakar M, Yıldız F, Özkütük A, Neşeli O, Kurhan E & Durdu O (2011). Sultanhanı Kervansarayı Fotogrametrik Rölöve Alımı ve 3 Boyutlu Modelleme Çalışması. 13. Türkiye Harita Bilimsel ve Teknik Kurultayı.

Yakar M, Orhan O, Ulvi A, Yiğit A Y & Yüzer M M (2015). Sahip Ata Külliyesi Rölöve Örneği. *TMMOB Harita ve Kadastro Mühendisleri Odası*, *10*.

*Mersin Photogrammetry Journal – 2021; 3(2); 53-60*

**Mersin Photogrammetry Journal**

https://dergipark.org.tr/en/pub/mephoj

**e-ISSN 2687-654X**

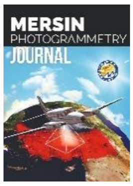


# Documenting historical monuments using smartphones: a case study of Fakih Dede Tomb, Konya

**Mustafa Emre Döş[1], Abdurahman Yasin Yiğit*[2], Murat Uysal[3]**

*[1]Hatay Mustafa Kemal University, Antakya Vocational School/Department of Architecture and Urban Planning, Hatay, Turkey*
*[2]Mersin University, Faculty of Engineering, Geomatics Engineering, Mersin, Turkey*
*[3]Afyon Kocatepe University, Engineering Faculty, Department of Geomatics Engineering, Afyonkarahisar, Turkey*

**Keywords**
Photogrammetry
Modelling
Historical Monuments
SFM
Smartphones

**ABSTRACT**

Cultural heritage and historical monuments are the memories of societies and enable future generations to learn about the past. However, historical monuments from the past to the present have been subjected to many destructions, natural or unnatural. Thanks to advances in technology, it is easier to document historical monuments using digital photogrammetric methods. Today, we see the methods used in documenting historical artifacts as traditional measurement, laser scanning, and photogrammetric methods or combinations of them. In this study, historical artifacts were tried to be documented through close-up photogrammetry methods, which is a sub-working area of photogrammetry, through images taken with non-metric cameras of smartphones that we use frequently in our daily lives. Planned geodesic measurement and photography should be done in order to perform three-dimensional (3D) modeling with close-up photogrammetry. During the study, the checkpoints were measured using geodesic methods on the historical monument and part of it was reserved for accuracy analysis. The tomb of Fakih Dede in Konya, which is an important point of visit in the region has been chosen.

## 1. Introduction

Cultural heritage has taken an important place in the culture and creativity of a society. Cultural heritages can be classified as public goods with their features (Yılmaz et al., 2000; Korumaz et al., 2011). Cultural and heritage properties provide certain benefits to the areas in which they are located, although there are not enough public resources for their maintenance and protection (Yakar et al., 2005; Alptekin et al., 2020; Polat et al., 2021a). Culture not only promotes economic development but can also be used as a means of transforming certain geographical areas. It, therefore, forms part of many local and regional economic development strategies (Alptekin et al., 2019; Polat et al., 2021b). Unfortunately, historical artifacts have been exposed to aging, humidity, dust, pressure, etc. over the years. They are exposed to irreversible deformation and damage caused by human beings as well as physical factors caused by the natural environment (Castellini et al., 2008; Lopez-Aparicio and Grašiene, 2013; Varas-Muriel et al. et al., 2014). Therefore, historical artifacts must be documented in order to be passed on to future generations. Documentation studies can form the basis for restoration projects of historical artifacts that have undergone deformation (Şenol et al., 2021).

Up-to-date and accurate information about architectural and structural features, geometric shapes, and materials are the most important bases for the restoration of historical monuments (Yakar et al. 2010). However, the original architectural drawings necessary for the restoration of historical monuments cannot be found or are of low quality. Therefore, it is vital to document historical artifacts and monitor their displacement and deformation (Şenol et al., 2020; Kaya et al., 2021; Sužiedelytė-Visockienė et al., 2015). The measurement of a structure with traditional methods is a costly and time-consuming task. Especially the high

* **Corresponding Author**

(mustafaemre.dos@mku.edu.tr) ORCID ID 0000-0002-7605-4270
*(ayasinyigit@mersin.edu.tr) ORCID ID 0000-0001-5202-4387
(muysal@aku.edu.tr) ORCID ID 0000-0001-5202-4387

**Cite this article**

Döş M E, Yiğit A Y & Uysal M (2021). Documenting historical monuments using smartphones: a case study of Fakih Dede Tomb, Konya. Mersin Photogrammetry Journal, 3(2), 53-60

**Research Article / DOI: 10.53093/mephoj.1026039**

**Received: 19/11/2021; Accepted: 14/12/2021**

parts of the structure are more difficult to access and measure. For this purpose, remote sensing and photogrammetric methods can be used (Ozimek et al., 2021; Yakar et al. 2015). The photogrammetry technique stands out as the most used technique, especially since it allows to the production of three-dimensional (3D) models from two-dimensional (2D) photographs taken with non-metric cameras.

Today, in the production of a 3D model, it is mainly obtained from active or passive sensors, which are non-contact systems based on light waves. We can currently distinguish four alternative methods for object and scene modeling:

- Image-Based Rendering is a preferred technique for rendering virtual views, which does not involve the creation of a geometric 3D model;
- Image-Based Modeling (e.g., photogrammetry), a commonly used method for geometric surfaces of architectural objects, precision terrain, and city modeling, and Cultural Heritage documents;
- Range Based Modeling (eg laser scanning) is also very common for non-expert users such as cultural heritage professionals;
- The combination of Image and Range Based Modeling, where both have advantages and disadvantages, and their integration can allow efficient and rapid generation of complete and detailed 3D models (Guarnieri et al., 2006).

More recently, experts in the documentation of cultural heritages have focused on the application of photogrammetric reconstruction, the documentation of historical artifacts (Di Angelo et al., 2021; Apollonio et al., 2021), and the documentation of complex buildings (Reinoso-Gordo et al., 2021; Donato et al. et al., 2019) have worked in many areas, from the documentation of historical landscape fragments (Bruha et al., 2020).

The integration of laser scanning technology and digital image photogrammetry enables the 3D digitization of architectural structures and elements. In this way, digital documentation and spatial information can be continuously monitored at different time intervals (Alkheder et al., 2009; Remondino, 2011; Pesci et al., 2013; Tapete et al., 2013). It creates a set of data points that can be converted into 3D point clouds required for the creation of 2D or 3D models with both technologies (Akman et al., 2010; Gruen and Akca, 2005; Yastikli et al., 2007). Although obtaining point cloud data using laser scanning is a faster technique, photogrammetric methods come to the fore due to their advantages such as affordability, limited accessibility of indoor building areas, limited portability, special expertise required, and other factors (Arias et al., 2006). ; Chandler et al., 2007; Martínez et al., 2013; Sužiedelyte-Visockiene et al., 2011).

These advantages of photogrammetry technology are based on the ability to work with newly developed algorithms. Photogrammetry, which has developed methodologically, has also been developed as data collection material. The first of these is the use of non-metric cameras. Thanks to the integration of non-metric cameras into smartphones, the photographic data obtained has become usable in photogrammetric evaluation. With the use of smartphones in this area, access to data collection tools has reached a high level. With the development of data collection materials, many people have started to use the photogrammetry technique with the photographic data obtained on smartphones and interesting results have emerged. Especially amateur users have found a place for themselves in a scientific study with the integration of photogrammetry technique with non-metric cameras without being aware of it.

In this study, images were taken with non-metric In this study, images were taken with non-metric cameras of smartphones, which we frequently use in our daily life, and a different study was carried out on the documentation of historical artifacts with the close-range photogrammetry method over these images. In the second part of the article, the results obtained from the field of study, the methods and materials used in the third part, and the results obtained in the fourth part are presented and finally, the results are discussed.

## 2. Study area

During the Karamanoğulları Principality period, the most important settlement area stands out as Konya. The political and cultural relations of the Karamanids and the Anatolian Seljuks began with the siege of Konya by Karamanoğlu Mehmed Bey in 1277. The urbanization activities of the Karamanoğulları Principality, which had an independent existence since the beginning of the 14th century, coincided with the first half of the 15th century. Urbanization activities in this process continued first in Ermenek, then in the centrum of Karaman and Konya. Karamanoğulları structures in Konya consist of small-sized mosques, tombs, darülhüffaz (the institution that trains Hafiz), and Turkish baths. According to the inscription of the Konya Ahmed Fakih Tomb, which constitutes our work, it was built in 1456 for Şeyh Fakih Pasha, the son of Isa. The tomb is located in the Karatay district of Konya province today. The mausoleum is structurally square prism type and has a single story. The structure is similar to Seljuk structures with a dome from the inside and an octagonal pyramidal cone/double-layered cover system from the outside. The tomb draws attention with the use of rubble, cut stone, brick, spolia, and tiles (Şaman-Doğan, 2009).

**Figure 1.** Fakih Dede Tomb north and south facade view

## 3. Material and method

Across studies, the use of a single stereo pair may be insufficient to reconstruct the complex structures of historic buildings. For this reason, almost all (80%) photographs should be used to cover the target object as a whole. Care should be taken to ensure regularity in selecting observation points and ensuring a conflict in the form of repeated photo coverage for at least 60% of the area of adjacent frames. Observations have shown that the optimal displacement angle between the sequential squares of the sequence is approximately 10o-15o when sensing the object from a circular orbit surrounding it (Asri & Çorumluoğlu, 2007; Skabek and Tomaka, 2014). This helps to improve accuracy when using images of a camera (smartphones) whose internal router is unknown or not calibrated. Therefore, bundle adjustment is a wide-spreading technique in today's terrestrial photogrammetry (Figure 2). Combines the application of semi-metric or even non-metric cameras, convergent photos, and flexible measurements in a common computer environment (Kuçak et al., 2016).

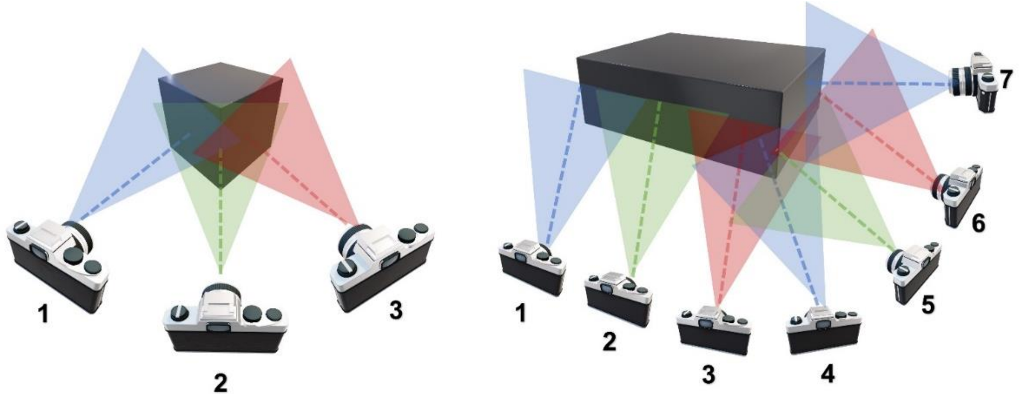


**Figure 2.** System of convergent taking of images for close-range photogrammetry

In this study, a total of 9 images were taken with a sufficient overlapping ratio, covering the historical building completely. The images were taken using the Huawei Mate 10 Lite android device shown in Table 1.

**Table 1.** Huawei Mate 10 Lite smartphone camera features

| Parameters | Value |
|---|---|
| Focal length | 27mm |
| Aperture | 2,20 |
| Sensor size | 18.46 x 27.69mm |
| Amount of pixels | 16MP |
| Weight | 164gr |
| Dimension | 156x75x7.5mm |

Planned geodetic measurement and photography should be done in order to make 3D modeling with the digital photogrammetric method. For geodetic measurement of control points on ancient artifacts to be used in the photogrammetric evaluation, first of all, a geodetic network that completely covers the object in all aspects should be established in such terrestrial photogrammetric and modeling studies. In this context, a geodetic network has been established in the local coordinate system that will completely cover the historical structure from all sides. When choosing the control points where the measuring device will be installed, locations that will see the structure fully are preferred. Considering the physical properties of the building surface, attention was paid to the selection of sharp lines and clear control points (Uysal et al., 2015). The Cygnus Topcon KS-102 reflectorless total-station was used to mark the closed polygon mesh and control points (Figure 3).

**Figure 3.** Cygnus Topcon KS-102 total-station

A closed polygon network was then established around the building, a total of 40 control points has been marked. For detail points, both target marks and points with natural sharp lines and characteristic features of the object were preferred. These data were primarily provided for reference in the process of merging the photographs in the software. In addition, these detail points are needed in order to examine the position accuracy of the points. 40 homogeneously distributed detail points were determined on the structure. Twenty-four of these points are marked for use in coordinating the 3D model, and 16 for accuracy analysis. After the measurement process was completed in the field, photography was done. Care has been taken to take the images with an overlay so that they can see the object from different angles. The workflow diagram of the basic workflow and Close-range photogrammetry technique used in the study for digital documentation is given in Figure 4.

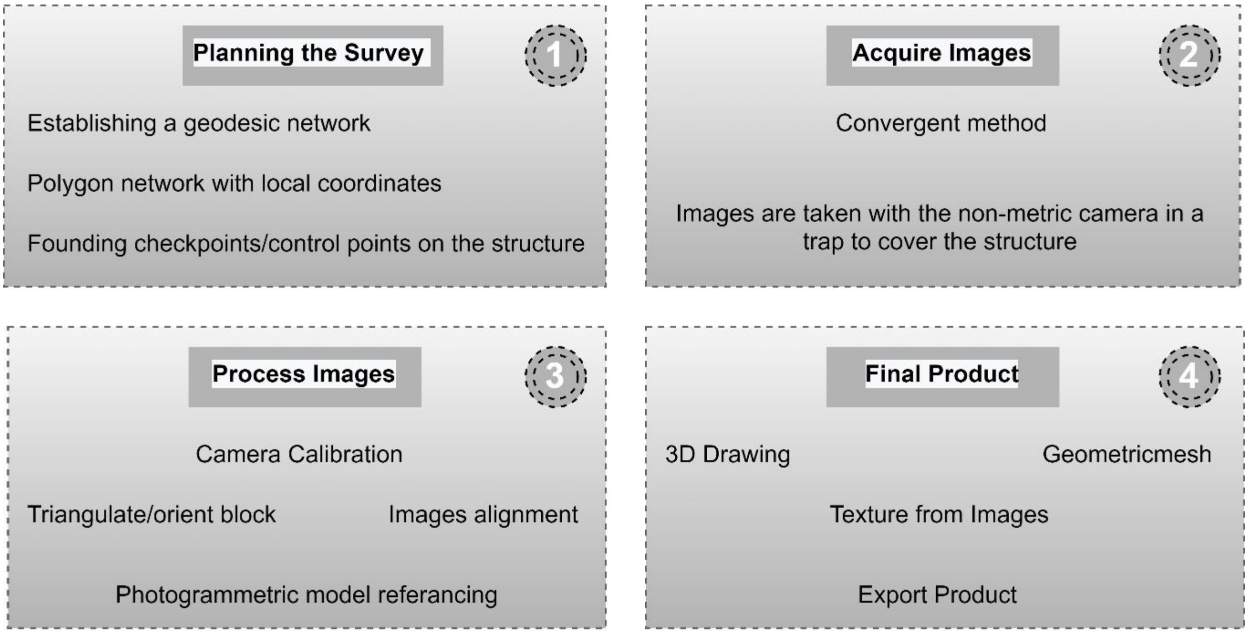


**Figure 4.** Basic workflow for Close-range Photogrammetry

The images and control points of the historical structure obtained as a result of the field studies were transferred to the PhotoModeler UAS software for digital evaluation. Since PhotoModeler software can perform mutual and absolute orientation at the same time, control points appearing in two or more images are marked (Yastiklı, 2013). After marking the checkpoints, one photograph was chosen as a reference and the other marked photographs were for the match of each checkpoint. Next, routing was done according to the package method in PhotoModeler software. After the orientation process, 3D model production started. Finally, texture data was added to the completed 3D model and the documentation of the historical building was completed.

## 4. Results

In the Photomodeler software, 9 ground-based photographs and 40 detail points were used with the non-metric camera on the smartphone. First, the photo and detail point data of the structure were introduced to the software. Detail points were manually marked on the photographs to be used, and merging and balancing were performed. After balancing the photographs, a 3-dimensional drawing of the basic skeleton of the building was obtained by drawing each detail one by one (Figure 5).

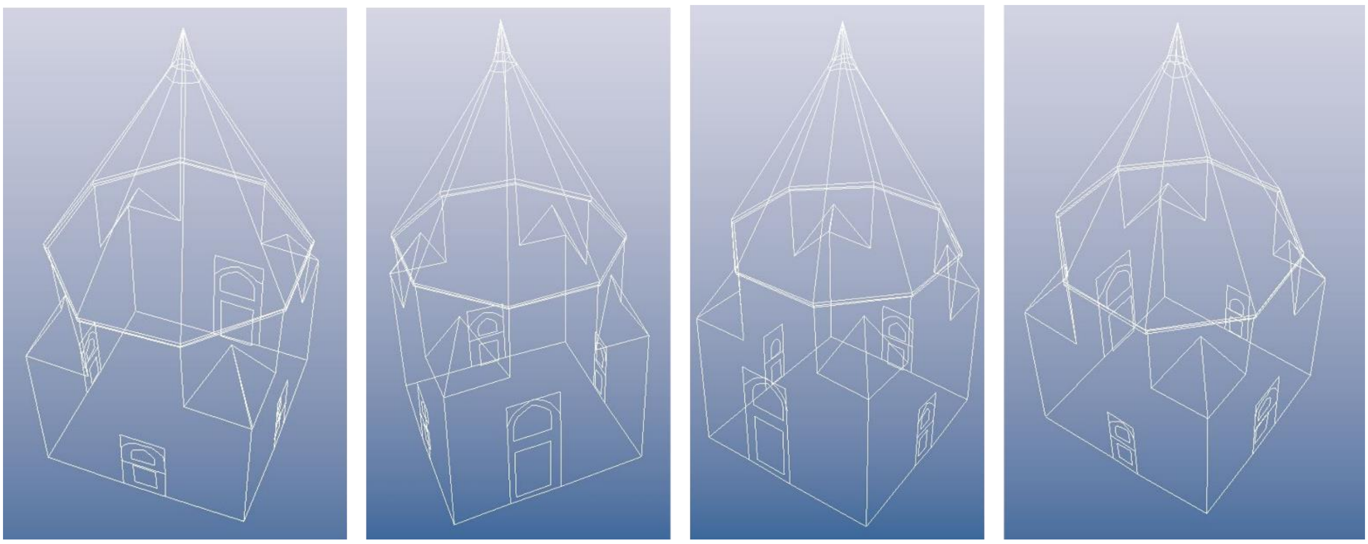

**Figure 5**. View of 3D Detail Drawing

By using these drawings as the basic skeleton, a solid model of the structure was covered (Figure 6). Finally, the surface of the solid model was dressed by means of photographs taken from the field, and a 3D model of the structure was textured (Figure 7).

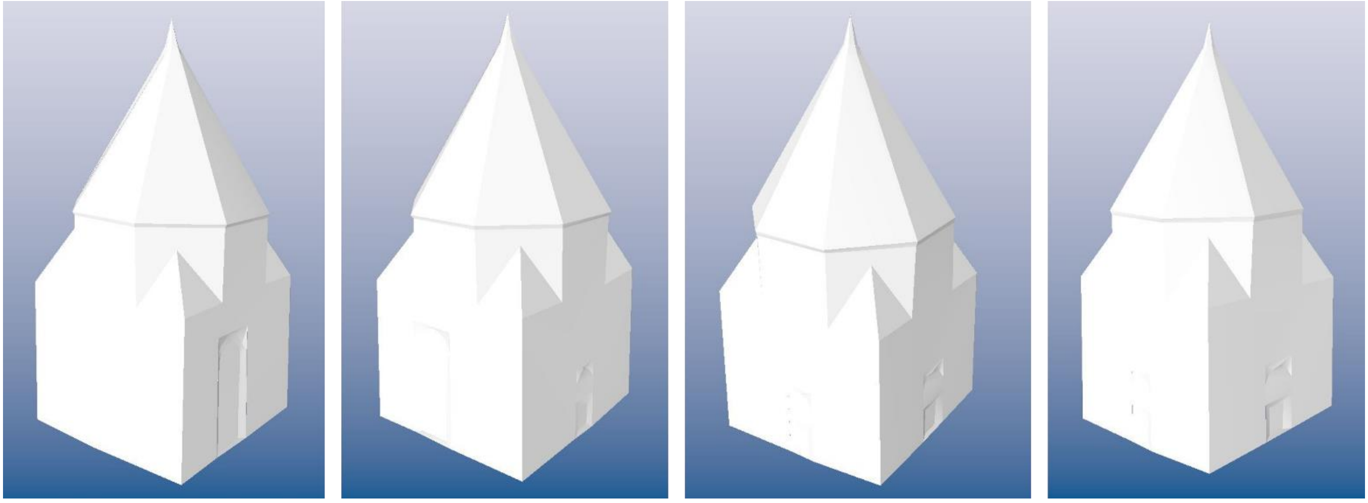

**Figure 6.** 3D Solid model

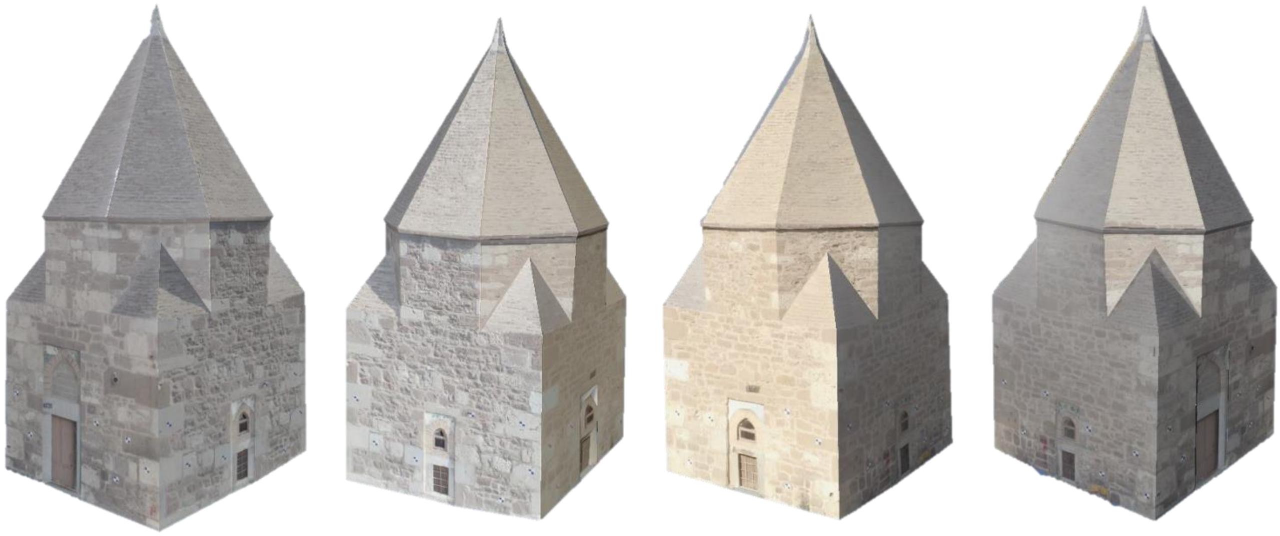

**Figure 7.** 3D photorealistic model view of Fakih Dede Tomb

Accuracy analysis was performed to detect the positional error for the 3D model obtained. For this process, the field coordinates obtained with the total-station measuring instrument and the test data obtained from the 3D model were evaluated. The coordinates taken with the measuring tool were accepted as the exact coordinates. By calculating the exact value and the value differences on the model, the mean square errors of the points in the x, y, z direction were calculated.

Detail points are needed to examine the position accuracy of the points. 40 homogeneously distributed detail points were determined on the structure (Figure 8). 16 of these points were used for accuracy analysis.

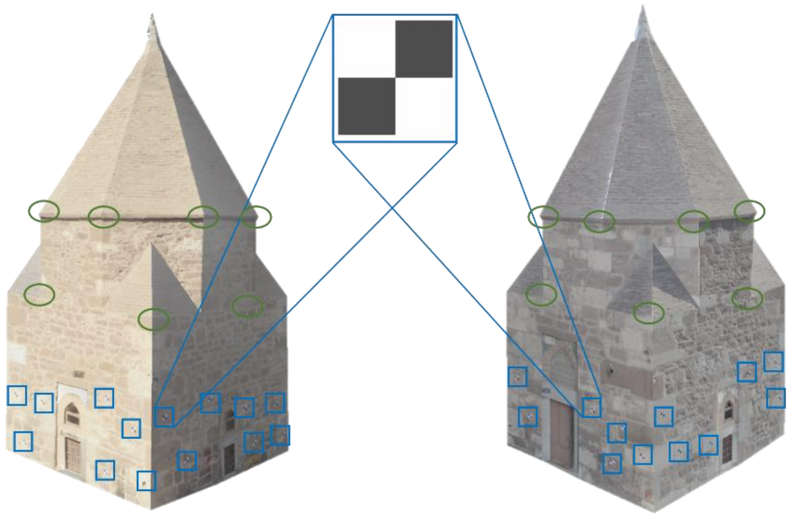

**Figure 8.** Display of control points used for photogrammetric process and accuracy analysis. The blue rectangles represent the paper target, and the green circles represent the distinctive characteristic points.

**Table 2.** Accuracy analysis of Control points

| Point Number | Vi (mm) | | | | Vi (mm) | | |
|---|---|---|---|---|---|---|---|
| | VxVx | VyVy | VzVz | Point N. | VxVx | VyVy | VzVz |
| *1* | 15 | 9 | 7 | *9* | 11 | 9 | -12 |
| *2* | -14 | 0 | 0 | *10* | -6 | -5 | 18 |
| *3* | 3 | 2 | 4 | *11* | 9 | -16 | 9 |
| *4* | -4 | -18 | 4 | *12* | -8 | -10 | 15 |
| *5* | -8 | -6 | -16 | *13* | 8 | -4 | -5 |
| *6* | 14 | 23 | -13 | *14* | -1 | 2 | 1 |
| *7* | -4 | 12 | 18 | *15* | -16 | 4 | 0 |
| *8* | -10 | 13 | 15 | *16* | -12 | 13 | -16 |

The spatial accuracy of the control points was calculated according to equation 1, taking into account the differences (vi) and the number of measures (n). The differences between the coordinate values measured by geodetic methods of 16 points reserved for accuracy analysis and the coordinate values read on the 3D model are presented in Table 2.

$$mX_0 = \sqrt{\frac{V_x V_x}{n-1}}, mY_0 = \sqrt{\frac{V_y V_y}{n-1}}, \ mZ_0 = \sqrt{\frac{V_z V_z}{n-1}} \quad (1)$$

When Table 2 is examined, it is seen that the 3D model is generally produced with high precision. The reason for the high error values in the partial axes of some points is thought to be due to the fact that the overlay ratios in the photographs are not constant and vary.

In addition, for the X, Y, Z position accuracy of the obtained model, mx, my, mz were calculated as 10.29, 11.41, 11.86 mm, respectively. If the position of the model is correct, it is calculated according to equation 2 and it is ± 1.94 cm.

$$m_{xyz} = \sqrt{mX_0 + mY_0 + mZ_0} \quad (2)$$

## 5. Conclusion

It is advantageous to use photogrammetric methods instead of traditional methods that require time-consuming and laborious measurements in the documentation of historical artifacts. However, photogrammetric methods have disadvantages such as expensive measuring instruments, high-dimensional data, and complex modeling processes.

In this study, the performance of photogrammetric methods in the documentation of historical artifacts by using non-metric cameras such as smartphones, which we use frequently in our daily life and which can be accessed more easily than alternatives, has been examined.

In order to examine the accuracy of the work, the differences between the control points and detail points measured with the total station were calculated and the precision of the model was found to be ±1.94 cm. Yakar and Bilgi (2020) study history by using mobile phones in III. They made 3D documentation of Ahmet Fountain. In their study, they found the 3D position accuracy to be ±2.56 cm.

It has been seen that the 3D model obtained in line with this study and the work done by Yakar and Bilgi can be used as a base for the documentation and protection of cultural heritage. These models play an important role in the restoration works, in determining the deformations that will occur on the historical artifacts and in monitoring the changes that occur on the artifacts in question. On the other hand, it is thought that mobile phones can contribute to the documentation of many cultural heritage works, especially since they have a large user base and their use does not require expertise.

## Author contributions

**Mustafa Emre Döş**: Conceptualization, Methodology, Software, Analysis; **Abdurahman Yasin Yiğit**: Data acquisition, Writing, Original draft preparation, Software, Validation, Visualization; **Murat Uysal**: Investigation, Writing-Reviewing and Editing.

## Conflicts of interest

The authors declare no conflicts of interest.

## References


Akman O., Bayramoğlu N., Aydin Alatan A., Jonker P. (2010). Utilization of Spatial Information for Point Cloud Segmentation, 3DTV-Conference 2010: The True Vision – Capture. *Transmission and Display of 3D Video, DOI: 10.1109/3DTV.2010.5506339.*

Al-kheder S, Al-shawabkeh Y & Haala N (2009). Developing a documentation system for desert palaces in Jordan using 3D laser scanning and digital photogrammetry. In *Journal of Archaeological Science, 36, 537-546*.

Alptekin A & Yakar M (2020). Mersin Akyar Falezi'nin 3B modeli. Turkey Lidar Journal, 2(1), 5-9.

Alptekin A, Fidan Ş, Karabacak A, Çelik M Ö & Yakar M (2019). Üçayak Örenyeri'nin yersel lazer tarayıcı kullanılarak modellenmesi. Turkey Lidar Journal, 1(1), 16-20.

Apollonio F I, Fantini F, Garagnani S & Gaiani M (2021). A Photogrammerty-Based Workflow for the Accurate 3D Construction and Visualization of Museums Assests. In *Remote Sensing, 13(3).*

Arias P, Ordóñez C, Lorenzo H & Herraez J (2006). Methods for documenting historical agro-industrial buildings: a comparative study and a simple photogrammetric method. In *Journal of Cultural Heritage, 7, 350-354.*

Asri İ & Çorumluoğlu Ö (2007). Büyük Objelerde Tarihi Dokümantasyon ve Tanıtım Amaçlı Gpssit Destekli Digital Fotogrametrik 3B Modelleme. TUFUAB IV. Teknik Sempozyumu, İstanbul.

Asri İ & Çorumluoğlu Ö (2014). Tarihi yerleşim alanlarının yersel fotogrametri yöntemi ile 3b modellenmesi: Santa harabeleri örneği, Uzaktan Algılama-CBS Sempozyumu (UZAL-CBS 2014), İstanbul, 1-8.

Castellini P, Abaskin V & Achimova E, (2007). Portable electronic speckle interferometry device for the damages measurements in veneered wood artworks. *Journal of Cultural Heritage, 9, 225-233.*

Chandler J H, Bryan P & Fryer J G (2007). The development and application of a simple methodology for recording rock art using consumer-grade digital cameras. In *Photogrammetric Record, 22, 10-21.*

Di Angelo L, Di Stefano P, Guardiani E & Morabito A E M (2021). A 3D Informational Database for Automatic Archiving of Archaeological Pottery Finds. In *Sensors, 21(3)*.

Donato E & Giuffrida D (2019). Combined Methodologies for the Survey and Documentation of Historical Buildings: The Castle of Scalea (CS, Italy). In *Heritage 2019, 2, 2384–2397.*

Gruen A & Akca D (2005). Least squares 3D surface and curve matching. In *ISPRS Journal of Photogrammetry and Remote Sensing, 59, 151-174.*

Guarnieri A, Remondino F & Vettore A (2006). Digital Photogrammetry and TLS Data Fusion Applied to Cultural Heritage 3D Modeling. *ISPRS Commission V Symposium, Image Engineering and Vision Metrologhy, September 25-27, 2006, Dresten, Germany*.

Kaya Y, Polat N, Şenol H İ, Memduhoğlu A & Ulukavak M (2021). Arkeolojik kalıntıların belgelenmesinde yersel ve İHA fotogrametrisinin birlikte kullanımı. Türkiye Fotogrametri Dergisi, 3 (1), 9-14. DOI: 10.53030/tufod.899089

Korumaz A G, Dülgerler O N & Yakar M (2011). Kültürel Mirasin Belgelenmesinde Dijital Yaklaşimlar. Selçuk Üniversitesi Mühendislik, Bilim ve Teknoloji Dergisi, 26(3), 67-83.

Kuçak R A, Kiliç F & Kisa A (2016). Analysıs of Terrestrıal Laser Scannıng and Photogrammetry Data For Documentatıon Of Hıstorıcal Artıfacts. *Int. Arch. Photogramm. Remote Sens. Spatial Inf. Sci., Xlıı-2/W1,155–158,Https://Doi.Org/10.5194/İsprs-Archives-Xlıı-2-W1-155-2016, 2016.*

López-Aparicio S & Grašiene R (2013) Screening indoor air quality evaluation in the Lithuanian theatre, music and cinema museum. *Journal of Environmental Engineering and Landscape Management. 21, 52-58.*

Martínez S, Ortiz J, Gil M L, Rego M T (2013). Recording complex structures using close range photogrammetry: The cathedral of Santiago de Compostela. In *Photogrammetric Record, 28, 375-395.*

Ozimek A, Ozimek P, Skabek K & Labedz P (2021). Digital Modelling and Accuracy Verification of a Complex Architectural Object Based on Photogrammetric Reconstruction. In *Buildings 11(5).*

Pesci A, Teza G, Bonali E, Casula G & Boschy E (2013). A laser scanning-based method for fast estimation of seismic-induced building deformation. In *ISPRS Journal of Photogrammetric and Remote Sensing, 79, 185-198.*

Polat N, Çokoğullu S, Memduhoğlu A, Ulukavak M, Şenol H İ, Oral M, Karaçizmeli M & Marangoz Ö (2021b). İha Fotogrametrisinin Arkeolojik Yüzey Araştirmalarina Katkilarinin İncelenmesi. TÜBA-AR Türkiye Bilimler Akademisi Arkeoloji Dergisi, (28), 175-186. DOI: 10.22520/tubaar.2021.28.009

Polat N, Önal M, Kaya Y, Memduhoğlu A, Kaya N, Ulukavak M, Mutlu S & Mutlu S (2021a). Harran Ören Yeri Kazısında Bulunan kabartma Yazıların Üç Boyutlu Olarak Modellenmesi. Bitlis Eren Üniversitesi Fen Bilimleri Dergisi, 10 (2), 594-601. DOI: 10.17798/bitlisfen.881781

Reinoso-Gordo J F, Gámiz-Gordo A & Barrero-Ortega P (2021). Digital Graphic Documentation and Architectural Heritage: Deformations in a 16th-Century Ceiling of the Pinelo Palace in Seville (Spain). In *ISPRS Int. J. Geo-Inf. 2021, 10, 85.*

Remondino F (2011). Heritage recording and 3D modeling with photogrammetry and 3D scanning. In Remote Sensing, 3, 1104-1138.

Şaman-Doğan N (2009). An Architectural Monument from Karamanoğlu Period: The Mausoleum of Fakih Dede in Konya. In *Hacettepe University Journal of Turkic Studies, 11(1), 91-108.*

Şenol H İ, Memduhoglu A & Ulukavak M (2020). Multi instrumental documentation and 3D modelling of an archaeological site: a case study in Kizilkoyun Necropolis Area. Dicle Üniversitesi Mühendislik Fakültesi Mühendislik Dergisi, 11 (3), 1241-1250. DOI: 10.24012/dumf.801662

Şenol H İ, Polat N, Kaya Y, Memduhoğlu A & Ulukavak M (2021). Digital documentation of ancient stone carving in Şuayip City. Mersin Photogrammetry Journal, 3 (1), 10-14. DOI: 10.53093/mephoj.899157

Skabek K & Tomaka A (2014). Comparison of photogrammetric techniques for surface reconstruction from images to reconstruction from laser scanning. *Theor. Appl. Informat. 2014, 26, 161–178.*

Sužiedelyte-Visockiene J, Kumetaitiene A & Bagdžiunaite R (2011). Accuracy analysis of different surface reconstruction modelling methods for heritage objects digitized considering photogrammetric data. In *Geodesy and Cartography, 37, 56-62.*

Suziedelyte-Visockiene J, Bagdziunaite R, Malys N & Maliene V. (2015). Close-Range Photogrammetry Enables Documentatıon of Envıronment-Induced Deformatıon of Archıtectural Herıtage. In *Envıronmental Engıneerıng and Management Journal, 14 (6). Pp. 1371-1381. Issn 1582-9596*

Tapete D, Casagli N, Guido L & Riccadro F (2013). Integrating radar and laser-based remote sensing techniques for monitoring structural deformation of archaeological heritage. In *Journal of Archaeological Science, 40, 176-189.*

Uysal M, Uslu A, Toprak A S & Polat N (2015). Menagas Pebble Stele Sample in Modeling 3 By Archaeological Photogrammetric Method. *TUFUAB VIII. Technical Symposium, pp: 252-254, Konya, Turkey.*

Varas-Muriel M J, Fort R, Martínez-Garrido M I, Zornoza-Indart A & López-Arce P (2014). Fluctuations in the indoor environment in Spanish rural churches and their effects on heritage conservation: Hygro-thermal and CO2 conditions monitoring. *Building and Environment*. *82, 97-109*.

Yakar İ & Bilgi S (2019). Mobil Telefonlar Kullanılarak Elde Edilen 3 Boyutlu Modellerin Kültürel Mirasın Korunması Kapsamında Kullanılabilirliği: Iı. Ahmet Çeşmesi Örneği. Türkiye Fotogrametri Dergisi, 1(1), 25-29.

Yakar M, Orhan O, Ulvi A, Yiğit A Y & Yüzer M M (2015). Sahip Ata Külliyesi Rölöve Örneği. *TMMOB Harita ve Kadastro Mühendisleri Odası*, *10*.

Yakar M, Yıldız, F & Yılmaz H M (2005). Tarihi Ve Kültürel Miraslarin Belgelenmesinde Jeodezi Fotogrametri Mühendislerinin Rolü. TMMOB Harita ve Kadastro Mühendisleri Odası, 10.

Yakar M, Yılmaz H M & Mutluoğlu Ö (2010). Comparative evaluation of excavation volume by TLS and total topographic station-based methods. Lasers in Eng,19, 331-345.

Yastikli N (2007). Documentation of cultural heritage using digital photogrammetry and laser scanning. In *Journal of Cultural Heritage, 8, 423-427.*

Yastıklı N (2014). Reverse Engineering Engineering Application of Earthly Photogrammetry. *UZAL-CBS Symposium, İstanbul, Turkey.*

Yılmaz H M, Karabörk H & Yakar M (2000). Yersel Fotogrametrinin Kullanim Alanlari. Niğde Üniversitesi Mühendislik Bilimleri Dergisi 4 (1), 1

**Mersin Photogrammetry Journal**

https://dergipark.org.tr/en/pub/mephoj

**e-ISSN 2687-654X**

# Detection of existing infrastructure lines with wearable laser scanners and making infrastructure map: a case of Mersin University

**Ali Ulvi*[1], Abdurahman Yasin Yiğit[2], Mehmet Özgür Çelik[2], Aydın Alptekin[3]**

[1]*Mersin University, Remote Sensing and Geographic Information Systems, Mersin, Turkey*
[2]*Mersin University, Geomatics Engineering Department, Mersin, Turkey*
[3]*Mersin University, Geological Engineering Department, Mersin, Turkey*

**Keywords**
WMLS
UAV
Photogrammetry
Point Cloud

**ABSTRACT**

Technological developments have shown themselves in the field of engineering as in every field. Wearable mobile laser scanner (WMLS) system is a technique based on simultaneous localization and mapping (SLAM) algorithm. This technique enables the creation of a map of an unknown environment bypassing with distance sensors while simultaneously determining the system located on the map. Due to the rapid progress in measurement technology, a heron WMLS has been used in the detection of underground lines. The point cloud of the roads was obtained with the laser scanner. Sewerage, water, and natural gas pipelines were determined through the point cloud. These determinations were checked with a Global Positioning System (GPS) device. As a result of this study, maps of the existing infrastructure lines in the campus were created.

## 1. Introduction

Infrastructure facilities are passed under roads and pavements, especially in city centers. Excavation demands that will arise due to the placement of new infrastructure lines, maintenance/repair and improvements of existing lines, capacity increases due to population increases that may arise over time, compulsory situations, etc. and cause various problems in terms of road superstructure (rigid, flexible) and road users (vehicle, pedestrian) (Karataş and Bıyık, 2015).

Information systems are needed in order to take fast and correct decisions as a result of infrastructure map production and to minimize the damages as explained in the aim of the project (Karataş and Bıyık, 2015). The understanding of infrastructure map production has developed with the construction of natural gas lines, however, the necessary importance has not been given fully. However, the production of maps for natural gas lines has also mobilized other infrastructure organizations. Intensive infrastructure works in our country in recent years damage the lines of other infrastructure institutions and these damages result in loss of life and property.

The reasons for these damages are infrastructure organizations do not use maps yet, the absence of maps of the region to be studied, relying on the memory of the people who do the work in the study area, incomplete and incorrect map measurements not updating the maps.

There are places where infrastructure maps are not available, not the Information System. Infrastructure maps are still in the minds of the craftsmen or on papers drawn randomly by underestimating the work done.

* **Corresponding Author**

*(aliulvi@mersin.edu.tr) ORCID ID 0000-0003-3005-8011
(abdurahmanyasinyigit@gmail.com) ORCID ID 0000-0002-9407-8022
(mozgurcelik@mersin.edu.tr) ORCID ID 0000-0003-4569-888X
(aydinalptekin@mersin.edu.tr) ORCID ID 0000-0002-5605-0758

**Cite this article**

Ulvi A, Yiğit a Y, Çelik M Ö & Alptekin A (2021). Detection of existing infrastructure lines with wearable laser scanners and making infrastructure map: a case of Mersin University. Mersin Photogrammetry Journal, 3(2), 61-68

**Research Article / DOI: 10.53093/mephoj.1036301**

**Received: 14/12/2021; Accepted: 24/12/2021**

The quality and efficiency of the infrastructure directly affects the quality of life of people, the healthy functioning of the social system, and the continuity of economic activities. The indicator of a nation's economic development is directly proportional to its infrastructure development. The infrastructure of a city is similar to the circulatory system of the human body. When even the slightest problem occurs in this system, it adversely affects other organs and systems, namely general health and living conditions.

Although there are many definitions of infrastructure, it is often associated with the phrase Public services. When it comes to public services, electricity, waste water, drinking water, natural gas, communication, etc., supplied by the relevant institutions (rather local governments) and developed when needed. Public services, which require a large amount of investment, produce solutions aimed at solving the problems of the public, and the planning, design, manufacturing and management processes are carried out or supervised by the relevant administration. In recent years, information technologies, which are the needs of the age, have been rapidly adopted and used by local governments. The inadequacy of traditional public administration instruments necessitates the effective and essential use of similar technologies in public administration.

Efficient and economical use of resources in the realization of infrastructure services requires effective planning and coordination. Coordinated planning and realization of infrastructure (drinking water, sewage, natural gas, electricity, communication, etc.) and road superstructure (asphalt, pavement, etc.) is of great importance in terms of preventing disruptions in pedestrian and pedestrian traffic and minimizing the damage to the environment.

In order to produce infrastructure maps, existing maps and orthophoto maps are needed. These maps can be produced with technical devices such as unmanned aerial vehicles, laser scanners, GPS and software that works in parallel with this hardware. Literature studies on these technical devices are shown below.

Heron Lite laser scanner is used in many fields, by different professional disciplines. There are studies examining working performance in different regions. Maset et al., (2021/a), investigated the usability and success of the wearable/portable heron lite mobile laser scanner (MLS) in two different outdoor environments. One of these environments; is a large and detailed building (university) that is shown among the standard uses of the heron lite scanner. The other one is the natural environment, where portable systems have not been used yet. The point clouds obtained from these two environments were compared with the reference models provided by traditional techniques (such as Terrestrial Laser Scanning (TLS) and Photogrammetry) and the results were investigated.

In another study conducted by Maset et al. (2021/b) the usability of the heron lite device was investigated in order to obtain reliable information about cities, public interior and exterior furnishings, and urban areas. The study was carried out in a closed indoor space.

Balenovic et al. (2021) compiled studies in which scanners were used to take forest inventory. They introduced handheld laser scanner systems and their features, and presented examples of their usability in forest inventory studies. Hyyppä et al., (2020) have used the UAV method in conjunction with a portable laser scanner to monitor changes in tree level in Boreal forests.

Volovodova & Kulik (2020), have studied the archaeological museum in the Matera region in the south of Italy. The usability of the Heron Lite Color laser scanner was investigated for monitoring cultural heritage structures and places. The main results obtained from their study are that the Heron Lite Color mobile laser scanning device can be used for three-dimensional modeling of cultural heritage objects in indoor spaces.

## 2. Unmanned aerial vehicle (UAV) photogrammetry and structure from motion (SFM)

With the development and use of UAVs and digital photogrammetric cameras in recent years, the usage of photogrammetry for map production has increased and has become a more cost-effective solution (Mirdan and Yakar, 2017). A dense point cloud can be obtained by directly connecting with ground control points (GCP) created with Global navigation satellite system (GNSS) measurement methods or by using RTK (Real Time Kinematic) GNSS systems on the UAV. Pond volume calculation (Alptekin and Yakar, 2020), rockfall site mapping (Alptekin et al. 2019), shoreline detection (Unel et al. 2020) and landslide site mapping (Kusak et al. 2021) are some of the examples.

While the dense point clouds could only be obtained with LIDAR (Laser Imaging Detection and Ranging) in the past, today the usage of UAVs allows to create high-accuracy orthophoto maps and digital surface model (DSM) (Gonçalves and Henriques, 2015; Peterman, 2015; Bui et al., 2017). The basis of data production in UAV photogrammetry is based on the central projection method. As in Figure 1, the rays coming from an object pass through the focal point in a linear way and fall on the projection plane. In this way, a projection of all objects in the image area is formed on this plane.

In recent years, with the development of UAV and SfM photogrammetry technology, the ability to obtain 3D models of the ground surface has been significantly enhanced (Fonstad et al. 2013; Hugenholtz et al. 2013; Tonkin et al. 2014; Clapuyt et al. and Van Oost 2015; Qu, Huang, and Zhang 2018).

SfM, a measurement method originating from computerized imaging techniques that are gaining popularity and is not very expensive (Westoby et al. 2012; Yakar et al. 2015), is based on the same principles as stereoscopic photogrammetry (Westoby et al. 2012; Barazzetti et al. 2011). In the SfM method, 3D structures are created from a series of overlapping images (Figure 2).

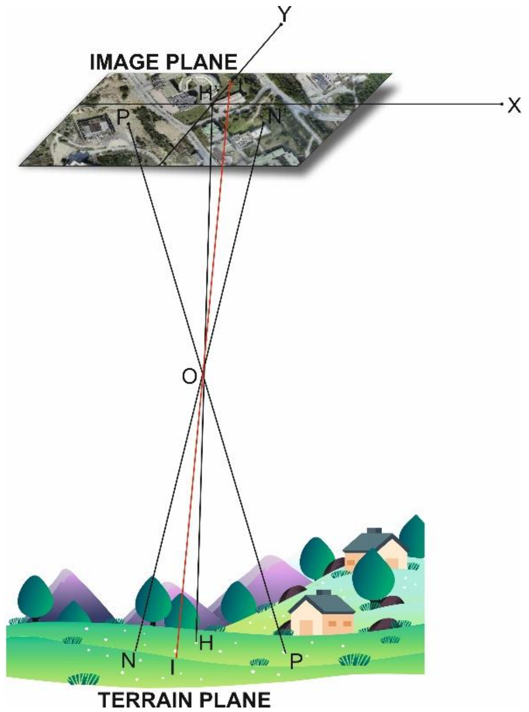


**Figure 1.** Relationship between ground and image coordinate system

O: Projection (Projection) center
P: Land point
H': Prime point
N': Rare point
H'OH: Principal axis (Uptake axis)
P'OP: Line of projection
I: Focal point

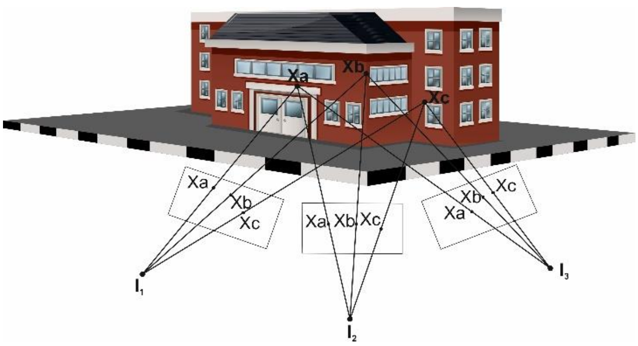


**Figure 2.** SfM diagram

## 3. Wearable mobile laser scanner (WMLS)

WMLS system is a technique, based on simultaneous localization and mapping (SLAM) algorithm. This technique enables the creation of a map of an unknown environment by passing with distance sensors while simultaneously determining the system location on the map.

These systems are capable of digitizing complex 3D scenarios without a global navigation satellite system (GNSS), thanks to SLAM algorithms (Bailay et al., 2006; Tang et al., 2015; Zeybek, 2021). The quality of the data depends on the rate of penetration and the distance to the object. These devices usually offer centimeter scale accuracy. Although these devices are more suitable for indoor use due to their higher productivity and efficiency than outdoor use, they have been successfully used for reconstructing outdoor scenarios such as cultural heritage, civil engineering and urban inventory.

Working with SLAM algorithm, the device receives data from its sensors (Inertial Measurement Unit (IMU) and odometry) in order to locate where it is in the environment. It uses this data to calculate the best estimate of where geometric objects in the environment (wall, floor, column, etc.) are located. Basically, the SLAM algorithm uses this data to detect the variability of the geometric objects (wall, floor, column, etc.) around a system to create a local coordinate map of the environment and to calculate the best estimate of where it is when determining its location.

## 4. Material and method

### 4.1. Ebee unmanned aerial vehicle

Fixed-wing ebee unmanned aerial vehicle was used within the scope of this study. The appearance of the UAV is shown in Figure 3 and its technical specifications are shown in Table 1. The technical specifications of the SODA camera used by Ebee UAV are shown in Table 2 and the residual view of the camera is shown in Figure 4.

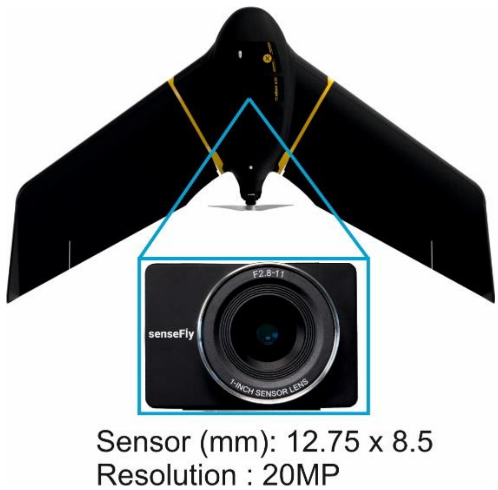


**Figure 3.** Ebee Plus and overview of the camera.

**Table 1.** Ebee Plus UAV technical specifications.

| Wingspan Weight | Camera | Control Software | | Maximum Flight Time Wing Resistance | |
|---|---|---|---|---|---|
| 110 cm | 1.1. kg | S.O.D.A. | Emotion 3 | 59 minute | Up to 45 km/h |

**Table 2.** Technical specifications of the camera used.

| Camera Model | Resolution | Focal Length | Pixel Size | Precalibrated |
|---|---|---|---|---|
| S.O.D.A.(10.6 mm) | 5472 x 3648 | 10.6 mm | 2.4 x 2.4 µm | No |

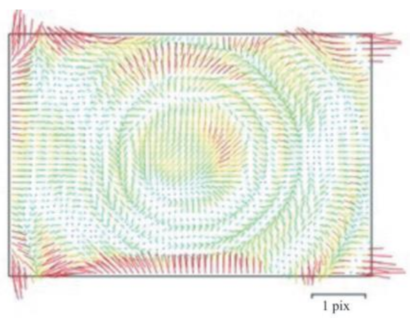


**Figure 4.** Image residuals for S.O.D.A. (10.6 mm)

## 4.2. Wearable Laser Scanner

The general view of the WMLS device used in this study is shown in Figure 5., and the technical specifications of the laser device is shown in Table 3.

**Figure 5.** Heron Lite Color Wearable laser scanner overview

The system shown in figure 6 has been taken into account for data collection and management with WMLS. In this context, it is possible to identify a number of methodological stages that characterize an audit: (i) research design (path planning); (ii) data collection (protocol and ground rules); (iii) post processing (SLAM algorithm for calculating sensor trajectory and mapping the environment); and (iv) cartographic product production (three-dimensional and two-dimensional digital models). Figure 6 summarizes the main steps of the applied methodology.

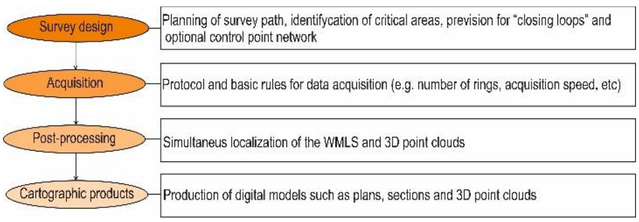


**Figure 6.** Methodological phases of the procedural pipeline for surveys with a WMLS

**Table 3.** Technical Performance Specifications of mobile LiDAR Gexcel Heron Lite Color provided by the manufacturer (URL-1).

| Technical Characteristic of Gexcel Heron Lite Color | Value |
|---|---|
| Brand and type | Velodyne VLP 16 |
| Measurement range | 0.4m - 100m indoor or outdoor |
| Measurement speed | Up to 300,000 points/second |
| Ranging Accuracy (for measurements of 10–100 m) | ±3 cm |
| Absolute accuracy [1 sigma in cm] | ±3 cm |
| Max survey resolution | ~ 2 cm |
| Field of view (vertical/horizontal) | 360°V / 360°H |

## 4.3. Data collection

### 4.3.1. UAV data collection

Seventeen Ground Control Points (GCPs) have been established in the campus area in order to obtain data with the UAV (Figures 7a and 7b).

(a) (b)

**Figure 7.** The study of establishing (a) and (b) Ground Control Points homogeneously on the campus area

While establishing the GCPs, attention was paid to distribute it homogeneously in the working area. After the completion of the GCP establishment process had completed, the coordinates were obtained with the SATLAB Global Positioning System (GPS) device in the ITRF96 datum system (Figure 8a / b).

(a) (b)

**Figure 8.** (a), (b). Coordinate obtaining of GCPs

The coordinates of the GCPs are shown in Table 4.

The flight was performed with 5 Ground Sampling Distance (GSD) and the flight altitude was 212 m. The flight duration lasted 120 minutes and a total of 1218 photographs were taken. Pre-flight preparatory work is shown in Figure 9 (a and b).

(a) (b)

**Figure 9.** (a) and (b) Pre-flight preparation procedures

**Table 4.** GCP koordinates

| Nokta | Y | X | Z |
|---|---|---|---|
| P.1 | 368698.660 | 4074215.516 | 137.115 |
| P.100 | 368716.714 | 4073616.490 | 101.422 |
| P.101 | 369168.474 | 4073638.694 | 104.272 |
| P.11 | 369080.534 | 4073986.770 | 107.766 |
| P.2 | 369599.618 | 4073675.892 | 80.785 |
| P.3 | 368948.478 | 4073093.430 | 102.594 |
| P.4 | 368306.151 | 4073348.508 | 101.630 |
| P.5 | 367949.748 | 4074037.107 | 135.519 |
| P.50 | 369545.940 | 4074179.552 | 82.676 |
| P.7 | 367699.989 | 4074761.942 | 198.432 |
| P.8 | 369225.418 | 4074742.175 | 110.503 |
| P.9 | 368882.376 | 4074800.483 | 115.018 |
| GCP1 | 368601.763 | 4073364.781 | 135.897 |
| GCP2 | 368503.024 | 4073705.701 | 149.072 |
| GCP3 | 368228.693 | 4074049.062 | 157.892 |
| GCP4 | 367924.452 | 4074293.231 | 176.264 |
| GCP5 | 368746.561 | 4073947.330 | 142.447 |

#### 4.3.2. Scanning process with Heron Laser Scanner

Some issues were taken into consideration in the field study with the WMLS system. First of all, position-based calibration of the WMLS system was performed before starting the measurement. In this section, the object or objects whose geometry is known to be considered are calibrated at the location. After the calibration process, the area to be scanned is measured at a constant speed. During the scanning, the following suggestions were taken into consideration to obtain accurate and sensitive data.

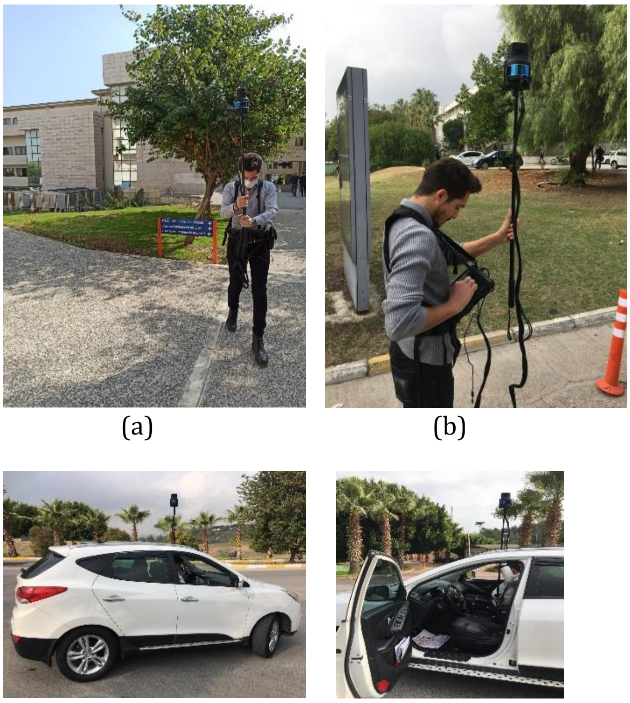

(a) (b) (c) (d)

**Figure 10.** (a) and (b) Scanning with the wearable laser scanner (c) and (d) using the laser scanner device in the vehicle

- Sudden movements during scanning cause deficiencies or distortions in the data to be obtained. For this reason, the route was followed by avoiding sudden movements.
- Moving objects (human, car, animal, etc.) cause corruption of the point cloud data to be created. In other words, it creates noise in the data. In such cases, it is necessary to avoid moving objects first, but in obligatory cases, the noises should be deleted when the data processing section is passed.
- In narrow areas, the system should not be kept at a distance where the scanned area can be seen.

Pictures of field scanning are shown in Figure 10. a.b.c.d.

In Figure 11a and b, the control of the measured underground lines was performed with a GPS device.

(a) (b)

**Figure 11.** (a) and (b) Coordinate control of underground lines with GPS device

## 5. Data evaluation

The orthophoto map obtained by the UAV was used as an auxiliary information source to provide a detailed representation of the project. Orthophoto map was produced with Agisoft software.

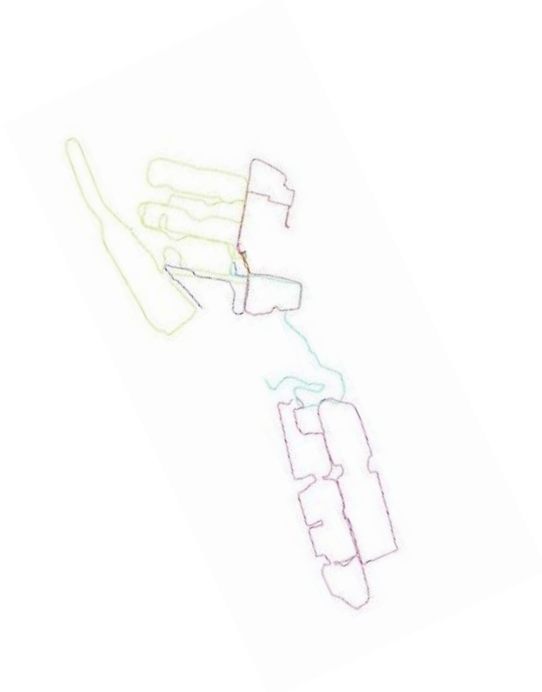

**Figure 12.** Trajectory measurements performed with the Heron device

The data obtained from the Heron device were evaluated in Gexcel software. As a result of the evaluation 703468676 points were produced. The route map of the underground lines was marked on the point cloud obtained with the Heron device (Figure 12). These markings were then matched with the orthophoto map obtained by the drone.

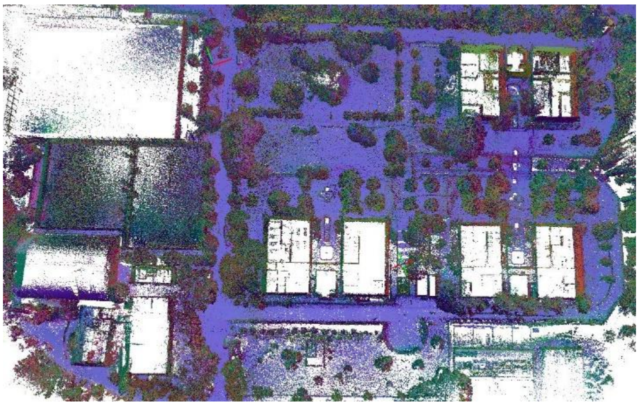

(a)

(b)

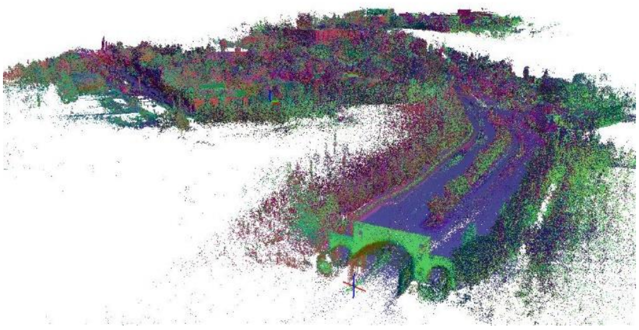

(c)

**Figure 13**. (a), (b), (c) Point cloud of Mersin University campus area produced by Heron mobile laser device

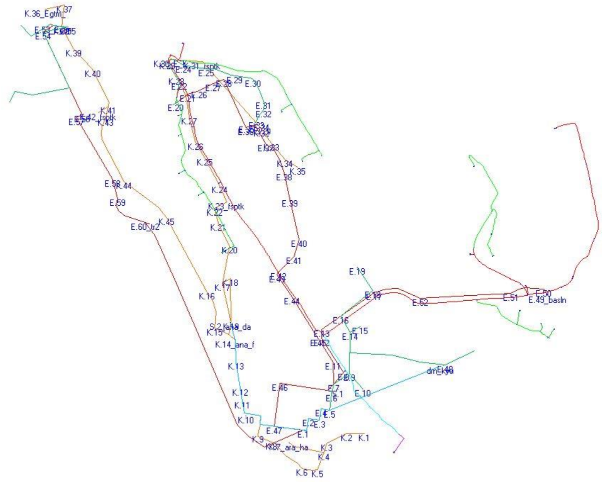

**Figure 14**. Route map created over the point cloud

**Figure 15**. Route map processed on orthophoto map

A legend, shown in Figure 16, has been created about which routes are being used in these mapping studies.

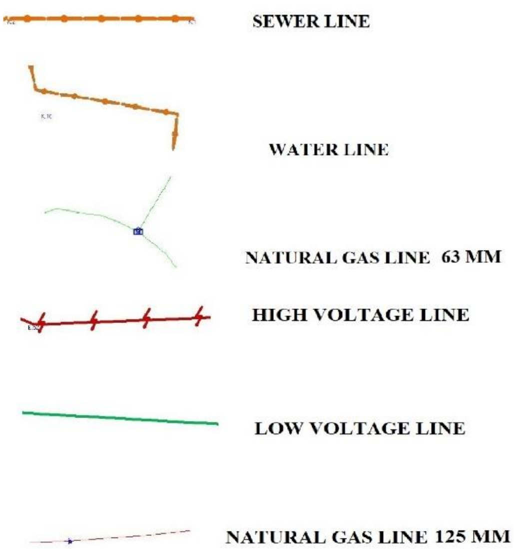


**Figure 16.** Legend representation of underground and surface lines

## 6. Conclusion

The rapidly developing laser scanning technology in recent years has become an acceptable and usable evaluation tool for many applications, as it offers powerful, practical, accurate and reliable solutions. As a result of the scanning process, in addition to the distance and 3D point location information, 3D models that give the scene appearance were obtained by combining the scanning data with the software. Wearable laser scanning technique provides a great advantage over classical measurement methods in obtaining accurate and reliable geometric and metric information by modeling detailed objects or complex scenes with very large data size faster.

Gexcel software caters to professional users. This software includes many more parameters, creates point cloud and mesh triangles without number limit, meets a wide variety of point cloud and mesh generation and editing commands, and supports many geometric applications, making this software among the most powerful 3D modeling software.

Technological developments have shown themselves in the field of engineering as in every field. Due to the rapid progress in measurement technology, heron WMLS has been used in the detection of underground lines (sewage, water and natural gas).

Especially the point cloud of the roads was obtained with the laser scanner. Sewerage, water and natural gas pipelines were determined through the point cloud. These determinations were checked with a GPS device. As a result of this study, maps of the existing infrastructure lines in the campus were created.

When this study is carried out in certain periods, the infrastructure maps will be constantly updated.

## Acknowledgement

This research was supported by Mersin University Scienific Research Project (BAP), Project no: 2020-1-AP5-4071

## Author contributions

**Ali Ulvi:** Conceptualization, Methodology, Software **Abdurahman Yasin Yiğit:** Data curation, Writing-Original draft preparation, Software, Validation. **Mehmet Özgür Çelik**: Software, Investigation **Aydın Alptekin:** Visualization, Writing-Reviewing and Editing.

## Conflicts of interest

The authors declare no conflicts of interest.

## References

Alptekin A & Yakar M (2020). Determination of pond volume with using an unmanned aerial vehicle. *Mersin Photogrammetry Journal*, *2*(2), 59-63.

Alptekin A, Çelik M Ö, Doğan Y & Yakar M (2019). Mapping of a rockfall site with an unmanned aerial vehicle. *Mersin Photogrammetry Journal*, *1*(1), 12-16.

Bailey T & Durrant-Whyte H (2016). Simultaneous localization and mapping (SLAM): Part II. IEEE Robot. Autom. Mag. 13, 108–117.

Balenović I, Liang X, Jurjević L, Hyyppä J, Seletković A & Kukko A (2021). Hand-Held Personal Laser Scanning – Current Status and Perspectives for Forest Inventory Application. Croatian Journal of Forest Engineering, 42(1), 165-183. https://doi: 10.5552/crojfe.2021.858

Barazzetti L, Binda L, Scaioni M, Taranto P (2011). Photogrammetric survey of complex geometries with low-cost software: Application to the 'G1' temple in Myson, Vietnam. Journal of Cultural Heritage, 12, 253-262, DOI: 10.1016/j.culher.2010.12.004

Bui D T, Long N Q, Bui X N, Nguyen V N, Van Pham C, Van Le C, Kristoffersen B (2017). Lightweight unmanned aerial vehicle and structure-from-motion photogrammetry for generating digital surface model for openpit coal mine area and its accuracy assessment. In International Conference on Geo-Spatial Technologies and Earth Resources, Springer, Cham, 17-33.

Clapuyt F V & Vanacker K Van Oost (2015). "Reproducibility of UAV-based Earth Topography Reconstructions Based on Structure-from-motion Algorithms." Geomorphology 260: 4–15. doi:10.1016/j.geomorph.2015.05.011.

Fonstad M A, J T Dietrich, B C. Courville J L, Jensen, and P. E. Carbonneau. (2013). Topographic Structure from Motion: A New Development in Photogrammetric Measurement. Earth Surface Processes and Landforms 38 (4): 421–430. doi:10.1002/esp.3366.

Gonçalves J A & Henriques R (2015). UAV photogrammetry for topographic monitoring of coastal areas. ISPRS Journal of Photogrammetry and Remote Sensing, 104, 101-111.

Hugenholtz C H K, Whitehead O W, Brown T E, Barchyn B J, Moorman A, Leclair K, Riddell & T Hamilton (2013). Geomorphological Mapping with a Small Unmanned Aircraft System (SUAS): Feature Detection and Accuracy Assessment of a Photogrammetrically-derived Digital Terrain Model. Geomorphology 194: 16–24. doi:10.1016/j.geomorph.2013.03.023.

Hyyppä E, Yu X, Kaartinen H, Hakala T, Kukko A, Vastaranta M & Hyyppä J (2020). Comparison of Backpack, Handheld, Under-Canopy UAV, and Above-Canopy UAV Laser Scanning for Field Reference Data Collection in Boreal Forests. Remote Sensing, 12(20), 3327. https://doi.org/10.3390/rs12203327

Karataş K & Bıyık C (2008/2). Jeodezi, Jeoinformasyon ve Arazi yönetimi dergisi, Sayı,99, 5-11

Maset E, Cucchiaro S, Cazorzi F, Crosilla F, Fusiello A & Beinat A (2021/a). Investigating The Performance of a Handheld Mobıle Mapping System in Different Outdoor Scenarios. XXIV ISPRS Congress. https://doi.org/10.5194/isprs-archives-XLIII-B1-2021-103-2021

Maset E, Scalera L, Beinat A, Cazorzi F, Crosilla F, Fusiello A & Gasparetto A (2021/b). Proceedings of I4SDG

Workshop 2021. I4SDG 2021. Mechanisms and Machine Science, vol 108. Springer, Cham. https://doi.org/10.1007/978-3-030-87383-7_32

Mırdan O & Yakar M (2017). Tarihi Eserlerin İnsansız Hava Aracı ile Modellenmesinde Karşılaşılan Sorunlar. Geomatik, 2 (3), 118-125. DOI: 10.29128/geomatik.306914

Peterman V (2015). Landslide activity monitoring with the help of unmanned aerial vehicle. The International Archives of Photogrammetry, Remote Sensing and Spatial Information Sciences, 40(1/W4), 215-218.

Qu Y, Huang J & Zhang X (2018). Rapid 3D Reconstruction for Image Sequence Acquired from UAV Camera. Sensors, 18: 225.

Tang J, Chen Y, Chen L, Liu J, Hyyppä J, Kukko A, Chen R (2015). Fast fingerprint database maintenance for indoor positioning based on UGV SLAM. Sensors, 15, 5311–5330.

Tonkin T N, Midgley N G, Graham D J & Labadz J C (2014). The Potential of Small Unmanned Aircraft Systems and Structure-from-motion for Topographic Surveys: A Test of Emerging Integrated Approaches at Cwm Idwal, North Wales. Geomorphology 226: 35–43. doi:10.1016/j. geomorph.2014.07.021.

URL-1: https://gexcel.it/en/solutions/heron-portable-3d-mapping-system (15.11.2021)

Ünel F B, Kuşak L, Çelik M Ö, Alptekin A & Yakar M (2020). Kıyı Çizgisinin Belirlenerek Mülkiyet Durumunun İncelenmesi. *Türkiye Arazi Yönetimi Dergisi*, *2*(1), 33-40.

Volovodova A V & Kulik E N (2020). Using Mobile Laser Scanning Data for Formation of Spatial Base for Monıtoring of Cultural Heritage Objects. UDC Handbook,528:7:528.8. https://10.33764/2618-981X-2020-6-1-80-86

Westoby M J, Brasington J, Glasser N F, Hambrey M J, Reynolds J M (2012). Structure-from-Motion' photogrammetry: A lowcost, effective tool for geoscience applications. Geomorphology, 179, 300-314, DOI: 10.1016/j.geomorph.2012.08.021

Yakar M, Orhan O, Ulvi A, Yiğit A Y & Yüzer M M (2015). Sahip Ata Külliyesi Rölöve Örneği. *TMMOB Harita ve Kadastro Mühendisleri Odası*, *10*.

Zeybek M (2021). Accuracy assessment of direct georeferencing UAV images with onboard global navigation satellite system and comparison of CORS/RTK surveying methods. Measurement Science and Technology